1 **Analysis of the variation of stable carbon isotopes in macroalgae communities from shallow**

2 **marine habitats in the Gulf of California ecoregion**

3

4 Macroalgal δ^{13}C variability in the Gulf of California

5

6 Roberto Velázquez-Ochoa[a], María Julia Ochoa-Izaguirre[b], Martín F. Soto-Jiménez[c*]

7 [a]Posgrado en Ciencias del Mar y Limnología, Universidad Nacional Autónoma de México, Unidad

8 Académica Mazatlán, Mazatlán, Sinaloa 82040, México

9 [c]Facultad de Ciencias del Mar, Universidad Autónoma de Sinaloa. Paseo Claussen s/n, Mazatlán,

10 Sinaloa 82000, México

11 [c]Unidad Académica Mazatlán, Instituto de Ciencias del Mar y Limnología, Universidad Nacional

12 Autónoma de México (UAM-ICMyL-UNAM), Mazatlán Sinaloa, 82040, México.

13

14 Correspondent author:

15 Telephone number: +52 (669) 9852845 to 48.

16 Fax number: +52 (669) 9826133

17 E-mail: martin@ola.icmyl.unam.mx

18

Abstract

The C isotopic composition in macroalgae (δ^{13}C) is highly variable and its prediction is very complex relative to terrestrial plants. To contribute to the knowledge on the variations and determinants of δ^{13}C-macroalgal, we analyzed a large stock of specimens varying in taxa and morphology and inhabiting shallow marine habitats from the Gulf of California Ecoregion featured by distinctive environmental conditions. A large δ^{13}C variability (-34.61‰ to -2.19‰) was observed, mostly explained on the life form (taxonomy, morphology and structural organization), and modulated by the interaction between habitat features and environmental conditions. The intertidal zone specimens had less negative δ^{13}C values than in subtidal zone. Except pH, environmental conditions of the seawater do not contribute to the δ^{13}C variability. Specimens of the same taxa showed δ^{13}C similar patterns, to increase or decrease, with latitude (21°-30°N). δ^{13}C-macroalgal provide information on the inorganic carbon source used for photosynthesis (CO_2 diffusive entry vs HCO_3^- active uptake). Most species showed a δ^{13}C belong into a range that indicates a mix of CO_2 and HCO_3^- uptake; the HCO_3^- uptake by active transport is widespread among GCE macroalgae. About 20-34% species depending on cutoff limits for CCM presence showed at least one specimen with δ^{13}C>-10‰, suggesting that potentially could have highly efficient CCM. Ochrophyta presented a high number of species with δ^{13}C>-10‰, suggesting widespread HCO_3^- use by non-diffusive mechanisms. Few species belonging to Rhodophyta relied on CO_2 diffusive entry (δ^{13}C<-30‰) exclusively. δ^{13}C provide useful information about the physiological and environmental status of macroalgae.

Keywords: δ^{13}C-macroalgal, carbon-concentrating mechanisms, CO_2 diffusive proxy

1. Introduction

By using sunlight, dissolved inorganic carbon (DIC) and inorganic nutrients, marine macrophytes produce biological compounds to maintain their metabolic functions, build basic structures, and to grow (Kirk, 2011). The light absorption properties of marine macrophytes are associated to the morphology or structural organization (e.g., thickness and form of the thallus containing the pigments) (Enríquez et al., 1994; Enríquez and Sand-Jensen, 2003). Even with the presence of a carbonate skeleton (e.g. calcium crystals in thallus/tissue act as a dispersive structure that enhance light absorption) and type and concentration of photosynthetic pigments (e.g., chlorophyll, carotenoid, and phycobilline) (Vásquez-Elizondo and Enríquez, 2017; Vásquez-Elizondo et al., 2017).

Macroalgae show a wide diversity of morphologies, structural organization (e.g., surface area/volume ratio), and various pigments. Based on these features, macroalgae can be classified into only three phyla, in agreement to the pigment contents in the thallus, or in dozens of groups considering morphologies and pigments (Littler and Littler, 1980; Littler & Arnold, 1982; Balata et al., 2011). For example, mixing of chlorophyll (*a*, *b*) and carotenoids are usually observed in Chlorophyta, chlorophyll (*a*, *c*) is dominant in Ocrophyta. Rhodophyta contains chlorophyll (*a*, *d*), carotenoid, and a mix of phycobilin (e.g. phycocyanin, phycoerthrin, allophycocyanin) (Bold and Wynne, 1978; Masojidek et al., 2004; Gateau et al., 2017). Both traits work as an excellent approximation to explain the fundamentals of metabolism, growth, zonation, and colonization (Littler and Littler, 1980; Littler and Arnold, 1982; Nielsen and Sand-Jensen, 1990; Vásquez-Elizondo and Enríquez, 2017).

Thallus thickness as the propriety of the morphology influences the diffusion boundary layer at the macroalgal surface, where the uptake of essential ions and dissolved gases by

3

66   macroalgae occur (Hurd, 2000; San-Ford and Crawford, 2000). In marine environments,

67   where pH~8.1±1, HCO_3^- accounting 98% of total DIC due the low diffusion rate of CO_2 in

68   seawater that results in a high HCO_3^- : CO_2 ratio (150:1) (Sand-Jensen and Gordon, 1984).

69   To overcome the limitations for growth imposed by low seawater CO_2 concentrations, most

70   of macroalgae have carbon concentrating mechanisms (CCMs) that increase internal carbon

71   inorganic concentration (near the site of RuBisCo activity (Giordano et al., 2005). For hence,

72   HCO_3^- uptake by most macroalgae is the principal inorganic carbon source for

73   photosynthesis, but a few species depend exclusively on to use of dissolved CO_2 that enter

74   by diffusion to the cells (Maberly et al., 1992; Beardall and Giordano, 2002; Raven et al.,

75   2002a, b; Giordano et al., 2005). So, macroalgal species with productivity limited by lacking

76   CCM's (have low plasticity for carbon inorganic forms uptake) seems to be restricted to

77   submareal habitats and composed mainly by red macroalgae (but without a morphological

78   patron clear) (Cornwall et al., 2015, Kübler and Dungeon, 2015). The rest of macroalgae with

79   CCM occupies from the intertidal to the deep submareal.

80   Nevertheless, marine ecosystems have many environmental factors, including habitat

81   features and environmental conditions in seawater that modify the main macroalgae

82   photosynthesis drivers (light, DIC, and inorganic nutrients). These factors could generate

83   negative consequences of their productivity, principally when they cause resources

84   limitation. Each factor vary from habitat to habitat (e.g. local scale: from intertidal to subtidal

85   and global scale: from temperate to tropical regions) and as in response to these

86   environmental changes, macroalgae can modulate their photosynthetic mechanism (Lapointe

87   and Duke, 1984; Dudgeon et al., 1990; Kübler and Davison 1993, Young et al., 2005). Such

88   modulation (up-and-down-regulation processes) implies a physiological acclimation,

89   focused to increase their photosynthetic activity, enhancing the transport of CO_2, HCO_3^- or

90   both into the cell and its fixation rates (Madsen and Maberly, 2003; Klenell et al., 2004; Zou

91   et al., 2004; Giordano et al., 2005; Enríquez y Rodriguez-Román, 2006; Rautemberger et al.,

92   2015).

93   The stable isotope composition of carbon on the thallus of marine macrophytes (referred as

94   $\delta^{13}C$) is a proxy used to identify CO_2 or HCO_3^- source in photosynthesis and infer the

95   presence or absence of CCM's (Maberly et al., 1992; Raven et al., 2002a). Also, $\delta^{13}C$ signal

96   in the algal thallus can be used as an indicator of the physiological state of photosynthetic

97   metabolism (Kim et al., 2014; Kübler and Dungeon, 2015).

98   First interpretations of $\delta^{13}C$ were in terrestrial plants leaves and were used to identify carbon

99   assimilation pathways due to differences in a large scale among them, where C_3 plants range

100   between -20‰ to -38‰, C_4 plants vary from -8‰ to -19‰, and CAM with an intermediate-

101   range from -11‰ to -34‰ (O'Leary, 1988). However, these classification ranges do not

102   apply in marine macrophytes, since virtually most of the marine plants have C3 pathway,

103   altough C4 co-existing features have been documented in some macroalgae species

104   (Kuppers, et al., 1978; Kremer 1981; Reiskind et al. 1988; Reiskind and Bowes 1991; Xu et.

105   al., 2013; Kustka et al., 2014). The photosynthetic pathways alterations can be stimulated by

106   great environmental changes in relation to adverse circumstances (Ehleringer et al., 1997;

107   Doubnerová and Ryslavá, 2011; Xu et. al., 2012, 2013) or to streamline carbon fixation under

108   excess of resources availability (Valiela et al., 2018). In marine environments, the

109   discrimination against the "heavier" and less abundant in nature carbon isotope (^{13}C), occurs

110   during the atmospheric CO_2 diffusion into the seawater and the posterior enzymatic

111   discrimination during it fixation into the cell (O'leary, 1988,1993; Marshal et al., 2007). This

112   last step is mainly related to the DIC acquisition mechanisms, which vary with taxonomy,

113   physiological and morphological features (Raven et al., 2002ab; Mercado et al., 2009,

114   Marconi et al., 2011; Hepburn et al., 2011; Fernandez et al., 2014, 2015; Rautemberger et al.,

115   2015; Stepien et al., 2015, 2016).

116   Consequently, $\delta^{13}C$ variability depends, in part, on the life form (taxonomy, morphology and

117   structural organization), but also is modulated by the interaction to environmental conditions

118   (light, DIC and nutrients). Thus, the prediction of the $\delta^{13}C$ variability in marine macrophytes

119   is very complex relative to terrestrial plants.

120   In this study, our objective was to investigate the contributions of life form, the changes in the habitat

121   features and environmental conditions, to the $\delta^{13}C$ macroalgal variability in communities in the Gulf

122   of California ecoregion (GCE). A second objective was to describe the proportion of species that

123   lacks CCM inferred by the $\delta 13C$ signal along and between the GCE bioregions. Finally, the third

124   objective was to explore the variability of $\delta^{13}C$ among the macroalgal morphofunctional groups and

125   latitude to find geographical patterns along GCE. Macroalgae as biomonitor constitute an efficient

126   tool in monitoring programs in large geographical regions (Balata et al., 2011) and environmental

127   impact assessments (Ochoa-Izaguirre and Soto-Jiménez, 2014).

128   To reach our objectives, we collected a large stock of macroalgae specimens of a diversity of species

129   characterized by a variety of morphological and physiological properties. Besides high diversity, in

130   terms of life forms, we selected a variety of shallow marine habitats along a latitudinal gradient in

131   the GCE for the sample collection, characterized by unique and changing environmental factors. The

132   GCE features abundant and diverse macroalgae populations, which are acclimated and adapted to

133   diverse habitats with environment conditions contrasting, determining the light, DIC and nutrients

134   availability.

135   **2. Materials and Methods**

2.1. Study area

The Gulf of California Ecoregion (GCE) is a subtropical, semi-enclosed sea of the Pacific coast of Mexico, with exceptionally high productivity being the most important fishing regions for Mexico and one of the most biologically diverse worldwide marine areas (Zeitzschel, 1969; Espinosa-Carreón and Valdez-Holguín 2007; Lluch-Cota et al., 2007; Páez-Osuna et al., 2017). GC represents only 0.008% of the area covered by the seas of the planet (265,894 km^2, 150 km wide and 1000 km long covering >9 degrees latitude) but has a high physiographic diversity and is biologically mega-diverse with many species endemic (Wilkinson et al., 2009; Espinosa-Carreón and Escobedo-Urías, 2017).

Regionalization criteria of the GCE include phytoplankton distribution (Gilbert and Allen, 1943), topography (Rusnak et al., 1964) and depth (Álvarez-Borrego, 1983), oceanographic characteristics (Roden and Emilson, 1979; Álvarez-Borrego, 1983; Marinone, 2003), biogeography (Santamaría-del-Ángel et al., 1994a), and bio-optical characteristics (Bastidas-Salamanca et al., 2014). The topography is variable along GCE, includes submarine canyons, basins, and variable continental platform. Besides, GCE presents complex hydrodynamic processes, including internal waves, fronts, upwelling, vortices, mixing of tides. he gulf's coastline is divided in three shores that include large rocky shores, long sandy beaches, and numerous scattered estuaries, coastal lagoons, and open muddy bays tidal flats, and coastal wetlands (Lluch-Cota et al., 2007).

GCE is different in the north and the south related to a wide range of physicochemical factors. The surface currents seasonally change direction and flow to the Southeast with maximum intensity during the winter and to the Northwest in summer (Roden (1958). The northern part is very shallow (<200 m deep averaged) divided in Upper Gulf, Northern Gulf and Grandes Islas. The

158 surrounding desserts largely influence this region (Norris, 2010) shows marked seasonal changes

159 in coastal seawater temperatures (Martínez-Díaz de León et al., 2006; Marinone, 2007). Tidal

160 currents induce a significant cyclonic circulation through June to September and anticyclonic from

161 November to April (Carrillo et al., 2002; Bray, 1988a; Velasco-Fuentes and Marinone, 1999;

162 Martínez-Díaz-de-León, 2001). The southern part consists of a series of basins whose depths

163 increase towards the South (Fig. 1). The southern region is influenced by typical

164 tropical/subtropical conditions that subject intertidal algae to desiccation primarily during summer.

165 The water column's physicochemical characteristics are highly influenced by the contrasting

166 climatic seasons in the G.C.E.: the dry season (nominally from November to May) and the rainy

167 season (from June to October). Annual precipitation (1,080 mm y-1) and evaporation (56 mm y-1)

168 rates registered during the past 40 years were 881±365 mm y-1 and 53±7 mm y-1, respectively

169 (CNA, 2012).

170 Previous macroalgae floristic studies of the CGE, report around 580 species, including 116 endemic

171 species (Norris, 1975; Espinoza-Avalos, 1993). Based on oceanographic characteristics (Roden and

172 Groves, 1959) and in the endemic species distribution (Aguilar Rosas and Aguilar Rosas, 1993), the

173 CGE can be classified into three phycofloristic zones: 1) First zone located from the imaginary line

174 connecting San Francisquito Bay, B.C. to Guaymas, Sonora, with 51 endemic species. 2) Second

175 zone with an imaginary line from La Paz bay (B.C.S.) to Topolobampo (Sinaloa) with 41 endemic

176 species. 3) Third zone located with an imaginary line from Cabo San Lucas (B.C.S.) to Cabo

177 Corrientes (Jalisco) with 10 endemic species. Besides, 14 endemic species are distributed throughout

178 the GCE (Espinoza-Ávalos, 1993). The macroalgal communities are subject to the changing

179 environmental conditions in the diverse habitats in the GCE that delimits their zonation, which

180 tolerate with a series of anatomical and physiological adaptations to water movement, temperature,

181   sun exposure and light intensities, low pCO_2, desiccation (Espinoza-Avalos 1993).

182   **2.1 Macroalgae sampling**

183   In this study, the GCE (21°-30°N latitude) was divided into six coastal sectors based on the three

184   phycofloristic zones previously described and continental coastline (Fig. 1a). In each sector,

185   representative marine ecosystems were selected and classified according to the localization along

186   the peninsula (P1-P3) or continental (C1-C3) coastline. In each selected ecosystem, representative

187   habitats were sampled based on the presence of macroalgae communities and their characterization.

188   In terms of substrate type (e.g., sandy-rock, rocky shore), hydrodynamic (slow to faster water flows),

189   and protection level (exposed or protected sites), and immersion level (intertidal or subtidal) (Fig.

190   1b).

191   Based on the local environmental factors, macroalgae specimens (4-5) of the most representative

192   species were gathered by hand (free diving) during low tide. A total of 809 composite samples were

193   collected from marine habitats along GCE coastlines. The percentages of specimens collected for

194   the substrate type were sandy-rock 28% and rocky shores 72% based on the habitat features. Related

195   to the hydrodynamic, 30% of the specimens were collected in habitats with slow to moderate and

196   70% with moderate to fast water movement. Regarding the protection level, 57% were exposed

197   specimens, and 43% were protected. Finally, with respect to the emersion level, 56% were intertidal

198   and 44% subtidal macroalgae organisms. About half of the protected specimens were collected in

199   isolated rockpools, which was noted.

200   In 4-5 sites of each habitat, we measured *in situ* the salinity, temperature and pH by using a calibrated

201   multiparameter sonde (YSI 6600V) and the habitat characteristics mentioned above noted. Besides,

202   composite water samples were collected for nutrient and alkalinity in the laboratory. Briefly, the

203 representative habitats were classified by pH levels in >9.0 "alkalinized", 7.9-8.2 'typical' and <7.9

204 "acidified". Based on temperature in colder <20ºC, typical 20-25ºC, and warmer >25ºC. 72% of the

205 specimens were collected at typical pH values, 22% in alkalinized and 6% in acidified seawater.

206 Regarding the temperature, about 55% of the specimens were collected at typical, 31% at warmer

207 and 14% at colder seawaters. Regarding salinity, most of the ecosystems showed typical values for

208 seawater (35.4±0.91 ups, from 34.5 to 36.1 ups). In this study, the collection surveys were conducted

209 during spring (March-April) and dry season (nominally from November to May) from 2009 to 2014.

210 Only in few selected ecosystems located at C1 and C2 sectors, one sampling survey was conducted

211 at the end of the rainy season (nominally from June to October in 2014). Thus, these ecosystems

212 were possible to include habitat with a salinity range varying from estuarine (23.5±3.0 ups) to

213 hypersaline (42.7±7.0 ups) values. These habitats were mainly isolated rockpools and only a few

214 were sites near tidal channels receiving freshwater discharges. 95% of the specimens were collected

215 at typical seawater salinity, and only 1.5 and 3.5% in estuarine and hypersaline environments.

216 Detailed information on the selected shallow marine ecosystems, habitat characterization and

217 environmental conditions is summarized in the inserted table in Fig. 1.

218 **2.2 Macroalgae processing and analysis of the isotopic composition of carbon**

219 The collected material was washed *in situ* with surface seawater to remove the visible epiphytic

220 organisms, sediments, sand and debris and then thoroughly rinsed with MilliQ water. The

221 composite samples were double-packed in a plastic bag, labeled with the locality's name and

222 collection date, placed in an ice-cooler box to be kept to 4ºC, and immediately transported to the

223 laboratory at UAS-Facimar in Mazatlán. In the field, sample aliquots were also preserved in 4%

224 v/v formaldehyde solution for taxonomic identification to the genus or species level (when

225 possible). The following GCE macroalgal flora identification manuals were consulted: Dawson

226 1944; 1954; 1956; 1961; 1962; 1963; Setchell and Gardner 1920; 1924; Abbott and Hollenberg

227 1976; Ochoa-Izaguirre et al., 2007; Norris, 2010.

228 In the laboratory, macroalgae samples were immediately frozen at -30ºC until analysis. Then,

229 samples freeze-dried at -38ºC and 40 mm Hg for 3 days, upon which they were ground to a fine

230 powder and exposed to HCl vapor for 4 h (acid-fuming) to remove carbonates and dried at 60ºC

231 for 6 h (Harris et al. 2001). Five milligrams aliquots were encapsulated in tin cups (5x9 mm) and

232 stored in sample trays until analysis. Macroalgae samples were sent to the Stable Isotope Facility

233 (SIF) at the University of California at Davis, CA, USA. Natural ^{13}C relative abundance relative to

234 ^{12}C in samples was determined with mass spectrometry, using a Carlo Erba elemental analyzer

235 attached to a Finnigan Delta S mass spectrometer equipped with a Europa Scientific stable isotope

236 analyzer (ANCA-NT 20-20) and a liquid/solid preparation unit (PDZ, Europa, Crewz, UK).

237 Isotope ratios of the samples were calculated using the equation δ (‰)=(R$_{sample}$/R$_{standard}$-1)]x1000,

238 where R=^{13}C/^{12}C. The R$_{standard}$ is relative to the international V-PDB (Vienna PeeDee Belemnite)

239 standard. During the isotopic analysis, the SIF lab used different certified reference materials (e.g.

240 IAEA-600, USGS-40, USGS-41, USGS-42, USGS-43, USGS-61, USGS-64, an USGS-65) for the

241 analytical control quality. The analytical uncertainties reported for the SIF lab was 0.2‰ for δ^{13}C

242 (https://stableisotopefacility.ucdavis.edu/13cand15n.html). We also included triplicate aliquots of

243 several specimens of the same species and condition, collected from one patch or attached to the

244 same substrate to assess the method error by sampling and processing procedural. The

245 methodological uncertainties were <0.4‰.

246 **2.3. Analysis of δ^{13}C-macroalgal variability**

247 To analyze the variability of δ^{13}C values in macroalgae, the specimens' were grouped according to

248   the following criteria: taxonomy (phylum, genus, and species) and morpho-functional groups (e.g.,

249   thallus structure, growth form, branching pattern, and taxonomic affinities; Balata et al. 2011;

250   Ochoa-Izaguirre and Soto-Jiménez 2015).

251   Sampled specimens belong to three phyla, 63 genera and 167 species. The phyla were identified:

252   Rhodophyta (53%), Ochrophyta (22%) and Chlorophyta (25%). Most representative genus (and

253   their species) were Ulva (U. *lactuca, U. lobata, U. flexuosa,* and *U. intestinalis*), Codium (*C.*

254   *amplivesiculatum* and *C. simulans*), Chaetomorpha (*C. antenina*), Padina (*P. durvillaei*), Dictyota

255   (*D. dichotoma*), Colpomenia (*C. tuberculata* and *C. sinuosa*), Sargassum (*S. sinicola* and *S.*

256   *horridum*), Amphiroa (*Amphiroa* spp.), *Spyridia* spp, *Polysiphonia* spp., *Gymnogongrus* spp.,

257   Gracilaria (*G. vermiculophylla, G. pacifica* and *G. crispate*), Hypnea (*H. pannosa* and *H.*

258   *johnstonii*) Grateloupia (*G. filicina* and *G. versicolor*), and Laurencia (*L. papillosa* and *L.*

259   *pacifica*). An analysis of the biogeographical diversity among coastline sectors evidenced that P3

260   (43 genera of 63, 68%) and C3 (63%) at north recorded the highest number of genus, followed by

261   C1 (38%) and P1 (29%) at south, and P2 (27%) and C2 (22%) at center of both GCE coastlines.

262   Same pattern was observed in the species richness, zones P3 (94 of 167 species, 56%) and C3

263   (52%) at north, C1 (34%) and P1 (25%) at south, and C2 and P2 (19-20%) at center.

264   In order to find a geographic pattern associated with the $\delta^{13}C$ signal of macroalgae in this study, and

265   because the thallus morphology has been related to photosynthetic activity (Littler and Littler 1980),

266   macroalgae were grouped according to their characteristics morpho-functional proposed initially by

267   Littler and Littler (1980) and modified by Balata et al., (2011). Not all morphofunctional groups and

268   taxon were present in every site during each sampling survey, and the sample size in each group

269   varied for taxa, location, and time. The morphofunctional groups identified were 21, of which the

270   most common were C-tubular (6 spp., n=69; C-Blade-like (6 spp, n=55); C-Filamentous uniseriate

271 (17 spp, n=49); C-Erect thallus (5 spp, n=33); O-Compressed with branched or divided thallus (19

272 spp., n=92); O-Thick leathery macrophytes (12 spp., n=104); O-Hollow with spherical or

273 subspherical shape (4spp, n=87); R-Larged-sized corticated (57 spp., n=225); R-Filamentous

274 uniseriate and pluriseriate with erect thallus (9 spp., n=48); and R-Larged-sized articulated corallines

275 (6 spp, n=17). The diversity, in terms of presence/absence of the morphofunctional groups, varied

276 among coastline sectors, higher in C3 (16 of 21, 76%) and P3 (71%) at the north, followed by C1

277 (57%) and P1 (48%) at the south, and C2 and P2 and (42-48%) at the center of both GC coastlines.

278 Detailed information on macroalgae specimens collected (ecosystem, habitat, number of composite

279 samples, morphological group and taxon) is given as Supplementary Information (Table SI-1).

280 A basic statistical analysis of δ^{13}C values in different macroalgae groups was applied for distribution

281 and calculation of arithmetic mean, standard deviation, minimum and maximum. Because not all

282 macroalgal species were present in sufficient numbers at different collection habitats, several

283 macroalgal groups were not considered for statistical analysis. Regarding the life form, we compared

284 among morphofunctional groups, taxon collected in the same habitat (within-subjects factor) by

285 multivariate analysis of variance. When differences were noted, a Tukey-Kramer HSD (Honestly

286 Significant Difference) test was performed. Besides, variations of δ^{13}C macroalgal in specimens of

287 the same morpho-functional and taxon collected in different habitats were also investigated with a

288 Kruskal-Wallis test.

289 In this study, the relationships between δ^{13}C with each independent variable related to the

290 inherent macroalgae properties (morphology and taxon), biogeographical collection zone

291 (GC coastline and coastal sector), habitat features (substrate, hydrodynamic, protection and

292 emersion level) and environmental conditions (temperature, pH and salinity) were examined

293 through simple and multiple linear regression analyses. Excepting temperature, pH, and

13

294 salinity, most of the independent variables are categorical independent variables. However,

295 these continue variables were also categorized, such as previously was described. Analyses

296 of simple linear regression were performed to establish the relationships between δ^{13}C-

297 macroalgal with each environmental parameter analyzed as possible driving factors (e.g.,

298 temperature, salinity, pH). Multiple linear regression analyses were conducted to evaluate

299 the combined effects of those independent variables (macroalgae properties, biogeographical

300 collection zone, habitat features, and environmental conditions) on the δ^{13}C-macroalgal. In

301 the multivariable regression model, the dependent variable, δ^{13}C-macroalgal, is described as

302 a linear function of the independent variables X_i, as follows: δ^{13}C-macroalgal $= a + b_1(X_1) +$

303 $b_2(X_2) + \ldots + b_n(X_n)$ (1). Where a, is regression constant (it is the value of intercept and its

304 value is zero); b_1, b_2, and b_n, are regression coefficients for each independent variable X_i.

305 From each one of the fitted regression models, we extracted the estimated regression

306 coefficients for each of the predictor variables (e.g., Bayesian Information Criterion (BIC),

307 Akaike Information Criterion (AIC), root-mean-square error (RMSE), Mallow's Cp

308 criterion, F Ratio test, p-value for the test (Prob > F), coefficients of determination (R^2) and

309 the adjusted R^2 statistics) (SAS Institute Inc., 2018). All regression coefficients were used

310 indicator of the quality of the regression (Draper and Smith, 1998; Burnham and Anderson,

311 2002). Kolmogorov-Simirnov normality test was applied for all variables and all were

312 normally distributed. Most of the δ^{13}C values in each group showed a normal distribution.

313 For all statistical tests, a probability $P<0.05$ was used to determine statistical significance.

314 The statistical analysis of the results was done using JMP 14.0 software (SAS Institute Inc.).

315

316 **3. Results**

3.1. δ¹³C-macroalgal variability in function of taxonomy and morpho-functional groups

The variability of $\delta^{13}C$ values in macroalgae was analyzed by taxon in terms of phylum, genus, species. and morphofunctional groups. Ochrophyta displayed the values from -21.5 to -2.20‰ (-12.55±3.77‰), significantly higher to Chlorophyta (-25.92 to -5.57‰, -14.55±3.04‰) and Rhodophyta (-34.61 to -4.55‰, -14.84±3.96‰) (Fig. 2a-c). The $\delta^{13}C$-macroalgal values (mean±SD) for genus of Chlorophyta, Ochrophyta and Rhodophyta (Fig. 2d-f) varied from -33.79±1.17‰ for *Schizymenia* to -7.86±0.73‰ for *Amphiroa*. Multiple comparisons among the genera more representative of each taxon showed the following order *Schizymenia < Polysiphonia < Ulva*, *Gracilaria* and *Spyridia* (-16.17±0.67‰ to -15.11±0.26‰) < *Gymnogongrus, Laurencia, Hypnea, Cladophora, Dictyota, Sargasumm, Chaetomorpha*, and *Grateloupia* (from -15.40±0.71‰ to -13.86±0.78‰) < *Codium* and *Padina* (-12.52±2.46‰ to -12.45±2.54‰) < *Colpomenia* and *Amphiroa* (-9.26±0.32 to -7.86±0.73‰). Aggrupation of $\delta^{13}C$ values based on morpho-functional features on macroalgae are graphed in Fig. 3. The most representative groups in the phylum Chlorophyta, varied from -15.83±0.37‰ for C-Tubular to -12.45±0.54‰ for C-thallus erect. The phylum Ochrophyta includes O-Thick leathery with the lowest mean (-14.79±0.30‰) and O-Hollow with a spherical or subspherical shape with the highest values (-9.26±0.33‰). For Rhodophyta, the lowest $\delta^{13}C$ values were observed for R-flattened macrophytes (-24.0±9.63) and highest for R-Larger-sized articulated coralline (-7.89±0.75‰). Significant differences were observed among groups, which were ordered as follows: R-flattened macrophytes<R-blade like < C-Tubular < O-Tick leathery and R-Large size corticated < C-Blade like and C-Filamentous uniseriate < C-Erect thallus and O-Compressed with branch < O-Hollow with spherical < R-Larger-sized articulated coralline.

By multiple comparison analysis of the same genus at different coastal sectors (Fig. 4), non-

340   significant differences were observed among coastal sectors for most of the genus, except for

341   *Amphiroa*, *Codium*, *Padina*, and *Spyridia* with δ^{13}C values systematically more negatives in

342   continental than peninsular coastline (C1-C3 > P1-P3). Also, lower δ^{13}C values were observed in the

343   C2 sector for most of the genus and higher at P1 and P3. Due to the strong influence of genera

344   composition on morphofunctional group, similar results were found, and the graph is no showed.

345   For the most representative species, a detailed comparative analysis of macroalgal δ^{13}C values was

346   also conducted and displayed on Table 1-3 for phyla Chlorophyta, Ochrophyta and Rhodophyta,

347   respectively. For *Codium*, *C. brandegeei* (11.82±1.24‰) and *C. simulans* (-11.43±2.20‰) showed

348   higher δ^{13}C values than *C. amplivesculatum* (-14.44±2.74‰). The three *Colpomenia* species had

349   higher δ^{13}C values than the other genera. *C. tuberculata* (-8.75±3.2‰) showed values significantly

350   higher than *Colpomenia* sp. (-10.97±3.65‰) and *C. sinuosa* (-10.18±2.95‰). The four-

351   representative species of *Gracilaria* showed comparable δ^{13}C values, averaging from -16.48±1.64‰

352   for *G. pacifica* to -15.48±2.43‰ for *Gracilaria* sp. Three representative species of *Hypnea* showed

353   non-significant δ^{13}C differences, varied from -16.4±1.75‰ for *H. spinella* to -14.95±2.36‰ for

354   *Hypnea* sp. two species represented Laurencia, *Laurencia* sp. (-12.90±1.22‰) higher than *L.*

355   *pacifica* (-14.9±2.20‰). Two species represented *Padina*, being *Padina* sp. (-11.10±1.53‰) higher

356   than *P. durvillaei* (-13.20±2.59‰). *Sargassum* was one of the most diverse genera studied with six

357   representative species. Based on the δ^{13}C values the species were ordered as follow: *S. horridum* =

358   *S. sinicola* = *S. johnstoniis* (-15.52±2.89 to -15.10±2.41‰) < *S. lapazeanum* (-14.49±1.59‰) =

359   *Sargassum* sp. (-14.25±2.36‰) < *S. herphorizum* (-13.65±1.63‰). *Spyridia* was represented by

360   *Spyridia* sp. (-17.06±1.20‰) and *S. filamentosa* (-15.86±3.83‰) without significant differences.

361   The six representative species of *Ulva* were divided in two morphological groups, filamentous and

362   laminates. Filamentous species that averaged -16.35±2.01‰ for *U. clathrata*, -16.03±3.64‰ for *U.*

363 *flexuosa*, -15.78±1.72‰ for *U. acanthophora* and -15.29±2.54‰ for *U. intestinalis* and Ulva

364 laminates that included *U. linza* (-15.56±2.44‰) and *U. lactuca* (-14.10±3.13‰). Non-significant

365 differences were observed between morphological groups and among species. An elevated intra-

366 specific variability, 11-28%, explains average overlapping.

3.2. Taxonomy versus habitat features

368 Variability of δ^{13}C values for the most representative genera was evaluated by multiple comparative

369 analyses in the habitat features' function, including the substrate, hydrodynamic, and emersion level.

370 Large δ^{13}C variability observed between specimens of the same genus collected in the different

371 habits does not show any significant pattern, and non-significant differences were observed. An

372 exception was observed with the emersion level (showed in Fig. 5), where intertidal specimens

373 recorded less negative values than subtidal in most macroalgae genus. For example, for

374 *Hydroclathrus* (intertidal -5.74±0.89‰; subtidal -11.46±5.93‰), *Amphiroa* (Intertidal -6.93±1.52;

375 Subtidal -9.91±6.14), *Hypnea* (intertidal -13.56±2.56‰; submareal -18.60±1.88‰), and *Laurencia*

376 (intertidal -13.49±1.36‰; subtidal -17.11±1.80‰). Exceptions were observed for *Polysiphonia*

377 (intertidal -19.74±2.27‰, subtidal -14.94±6.69‰), *Spyridia* (intertidal -16.97±3.33‰, subtidal -

378 13.21±0.73‰) and *Colpomenia* (Intertidal -9.41±3.41‰, subtidal -7.76±1.34‰).

3.3. Taxonomy versus environmental conditions

380 Non-significant differences were observed for the same genera at different temperatures ranges,

381 except for *Grateloupia* (cold, -19.28±4.70‰, typical -14.45±2.23‰, warm -14.57±2.25‰) and

382 *Polysiphonia* (cold, -21.05±0.46‰, typical -18.12±5.54‰, warm -17.96±2.38‰) with more

383 negative values in colder than warmer waters. Significant differences were observed in δ^{13}C values

384 in macroalgae specimens from different genus in the same temperature range. For example,

385   *Colpomenia* (cold -8.34±2.43‰, typical -9.47±3.77‰, warm -9.22±2.64‰), *Codium* (cold -

386   11.98±1.91‰, typical -12.54±3.01‰, warm -13.61±0.62‰) and *Padina* (cold -11.34±2.55‰,

387   typical -11.88±1.76‰, warm -13.42±2.77‰) (Fig. 6a), was less negative than the other genus.

388   Overall, more negative δ^{13}C values in macroalgae specimens' values of the same genus were

389   observed at continental (C2) compared to peninsular CG coastline (P1-P3), and more negative

390   southward than northward.

391   Significant differences were observed among genus related to the pH level at seawater (Fig. 6b).

392   Typical pH seawater, *Amphiroa* (-8.80±5.44) and *Colpomenia* (-10.29±3.66‰) were 1-2‰ more

393   negatives than in alkaline waters, while *Ulva* (-15.08±2.47‰) and *Spyridia* (-15.34±2.12‰) were 3-

394   5‰ less negative than in acidic waters. *Amphiroa* and *Colpomenia* were not collected in acidic water

395   and neither *Spyridia* in alkaline waters to compare. Others genus also showed extremes values

396   between alkaline (*Tacanoosca* -7.60±1.01‰) and acidic waters (*Schizymenia*, -32.96±2.01‰). The

397   following order was observed in the genus collect at the three pH ranges: alkaline > typical > acidic.

398   Significant differences were observed for genus *Ahnfeltiopsis, Caulerpa, Gymnogongrus, Padina*,

399   and *Ulva* with higher values at alkaline than in acidic waters. Values of δ^{13}C for specimens of the

400   same genus collected at typical pH waters are mostly overlapped between those for alkaline and

401   acidic seawaters. Non-significant differences in δ^{13}C values were observed for *Grateloupia, Hypnea,*

402   and *Polysiphonia* concerning pH type waters.

403   Regarding the δ^{13}C variability for all data set in response to temperature and salinity, non-

404   significant trend was observed between δ^{13}C-macroalgal in function of both parameters. A poor

405   bivariate correlation, but significant, was observed between of δ^{13}C with pH ($R^2 = 0.04$) (Fig. 7).

406   **3.4. Variation latitudinal of δ^{13}C-macroalgal**

407   The δ^{13}C-macroalgal variation in the GCE biogeography was evaluated by an analysis of regression

408   linear between δ^{13}C values along the nine degrees latitude in both GC coastlines. A non-significant

409   latitudinal trend was observed for datasets, but for the three taxa's most representative genera, δ13C

410   values correlated with latitude (Fig. 8a-f). In Chlorophyta, with the higher genera number, δ^{13}C

411   values increased with latitude (Fig. 8a) with a weak but significant correlation. Contrarily, in

412   Ochrophyta (Fig. 8b) and Rhodophyta (Fig. 8c) specimens, the δ^{13}C values decreased with latitude.

413   Significant correlations ($p<0.001$) were observed for δ^{13}C-macroalgal versus latitude in the most

414   representative morphofunctional groups. Representative morphofunctional groups of Chlorophyta

415   (e.g., C-Tubular, C-Filamentous uniseriate, Fig. 8d) showed a positive correlation, while those

416   belonging to Ochrophyta (e.g., O-thick leathery; Fig. 8e) and Rhodophyta (e.g., R-large sized

417   corticated.; Fig. 8f) showed a negative trend with latitude.

418   **3.5. Analyses of δ^{13}C macroalgal variability**

419   An analysis of the effects, independent and combined, on the δ^{13}C-macroalgal variability

420   related to life form and environmental factors, was conducted. Firstly, simple linear regression

421   analyses were performed to evaluate the dependent variable's prediction power (δ^{13}C-

422   macroalgal) in the function of several independent variables controlling the main macroalgae

423   photosynthesis drivers (light, DIC and inorganic nutrients). Regression coefficients were

424   estimated for each fitted regression model, which are used indicator of the quality of the

425   regression (Draper and Smith, 1998; Burnham and Anderson, 2002) as was described in

426   Methods; however, our results description focused on the coefficients of determination (R^2 and

427   adjusted R^2). The coefficient R^2 describes the overall relationship between the independent

428   variables X_i with the dependent variable Y (δ^{13}C-macroalgal), and it is interpreted as the % of

429   contribution to the δ^{13}C variability. While the adjusted R^2 statistics compensate for possible

430   confounding effects between variables.

431   Results of the analysis of the relationships between δ^{13}C with each independent variable are

432   summarized in Table 4. Regarding the inherent macroalgae properties, Phyla explain only

433   7% of the variability, the morphofunctional properties 35%, and taxon by genus 46%, and by

434   species 57%. In terms of GC coastline (continental vs. peninsular) and coastal sectors (C1-

435   C3 and P1-P3), the biogeographical collection zone explained a maximum 5% of the

436   variability. Related to the habitat features, only emersion level (6%) contributed to the δ^{13}C

437   variability. The contribution of the seawater's environmental conditions was marginal for pH

438   (4%) and negligible for temperature and salinity. A marginal reduction in the percentage of

439   contribution was observed for Phyla (1%) and morphofunctional properties (1%), but

440   significant for genus (5%) and species (10%).

441   Multiple regression analyses were also performed to interpret the complex relationships

442   among δ^{13}C-macroalgal, considering the life form (morphofunctional and taxon by genus)

443   and their responses to environmental parameters. Results for the fitted regression models

444   performed for morphofunctional groups (Table 5) and genus (Table 6), evidenced that the

445   effect of the coastal sector and pH ranges on the δ^{13}C-macroalgal increased the % of

446   contribution in 9-10% each one. The emersion level increased in 5-6% the contribution

447   respect to individual effect of morphofunctional group and genus, the temperature and pH in

448   1 and 3%, respectively, while salinity decreased in 1-2%. Adding the effect of the

449   biogeographical collection zone, represented by coastline sector, to those for morpho-

450   functional group (Table 5) and genus (Table 7) a notable increase of 11-12% was observed.

451   The full model considering the combined effect of the coastline sector + Habitats features for

452   Morphofunctional group or Genus (Table 7), showed R^2 of 0.60 and 0.71. In contrast,

453   Coastline sector + Environmental conditions + Morphofunctional group or Genus the R^2

454   increased to 0.62 and 0.72, respectively. The interactive explanations of environmental

455   factors increased the explanation percentage of $\delta^{13}C$ variability; however, these contributions

456   were significantly lower than the explained by life forms, such as the morphofunctional

457   properties and taxa by genus and species.

458   The combined effect of environmental condition on the $\delta^{13}C$ variability was tested for the best-

459   represented morphological groups and genus. Results evidenced that 9 of 21 morphological groups

460   showed significant effects on the $\delta^{13}C$ variability (Table 8), five increasing and four decreasing the

461   model constant of $\delta^{13}C$=-14.21‰. For example, for the O-Hollow with spherical or subspherical

462   shape (+4.96‰) and R-Larger-sized articulated corallines (+6.32‰) the predicted values are -

463   7.89±0.80‰ and -9.25±0.47‰, while for R-Filamentous uniseriate and pluriseriate with erect thallus

464   (-2.15‰) and C-Tubular (-1.62‰) are -16.36±0.55‰ and -15.83±0.50‰, respectively. Regarding

465   taxon, a significant effect was observed only in 13 genera, including *Colpomenia* (+5.45‰),

466   *Amphiroa* (+6.84‰), and *Padina* (+2.19‰) increasing the signal, and *Polysiphonia* (-3.75‰),

467   *Gracilaria* (-0.89‰), and Spyridia (-1.46‰) decreasing the signal of the model constant (Table 9).

468   In 33 species was observed a significant effect on the $\delta^{13}C$ variability, including *C. tuberculate*

469   +5.87‰, *C. sinuosa* +4.42‰, *H. pannosa* +4.42‰, *H. johnstonii* +4.42‰, and *Amphiroa spp.* (+4.42

470   to 8.20‰) increasing the model constant $\delta^{13}C$= -14.59‰, and *Spyridia* sp. (-2.46‰), *G. filicina* (-

471   2.37‰), *P. mollis* (-5.22‰) and *S. pacifica* (-19.19‰) (Table 9).

472

473   **4. Discussions**

4.1. Relationship among taxonomy and habitat with δ¹³C signal

Our analyses showed high variability in the $\delta^{13}C$ signal in the large inventory of macroalgae collected along GCE coastline for five years. Most authors studying the isotopic composition of C in these organisms have reported the high isotopic variability, which has been attributable to the taxon-specific photosynthetic Ci acquisition properties (Raven et al., 2002, Mercado et al., 2009, Marconi et al., 2011, Stepien, 2015). Following the mechanistic interpretations of $\delta^{13}C$ signal for algal thallus, values of $\delta^{13}C$ more negative than -30‰ indicate that photosynthesis is exclusively dependent on CO_2 diffusion (absence of CCM), whereas values above -10‰ indicate non-diffusive Ci transport mechanism (HCO_3^- users by the presence of CCM; Maberly et al., 1992; Raven et al., 2002). To interpretate our results, no considerate the CO_2 leak out inside the cell could occur and change the cutoffs for CO_2 or HCO_3^- users (Sharkey and Berry, 1985; Raven et al., 2005).

In our study, 84% of the analyzed specimens belong into the intermediate range between -30‰ and -10‰, averaging -14.05±3.98‰, which is slightly higher than the global mean for intertidal macroalgal -17.35±0.43‰ based on the meta-analysis of macroalgal $\delta^{13}C$ compiled by Stepien (2015). The apparent differences in the $\delta^{13}C$ averages can be related to the organism origin, mostly from temperate and polar marine ecosystems (142 sampling sites temperate, eight sites from tropics and six from polar zones) in the Stepien (2015) compilation concerning the subtropical marine ecosystems in our study. Our global mean includes the specimens collected at submareal and intertidal habitats, because non-significant differences were observed in most of macroalgae groups.

These results suggest that macroalgal communities from subtropical marine ecosystems record higher values than communities from temperate. Seawater from temperate zones has more CO_2 dissolved availability, which results in more negative carbon isotopic values in macroalgae when the

496   Ci is incorporated into the tissue (Raven et al., 2002ab). $\delta^{13}C$ values evidence that most of the

497   sampled macroalgae in our study have an active CCM to fix involves the direct use of HCO_3^- with

498   little CO_2 diffusive uptake (Giordano et al., 2005; Hopkinson et al., 2011; Hopkinson, 2014; Raven

499   and Beardall, 2016). However, based only on the $\delta^{13}C$ values, it is not possible to discern that CCM

500   type is expressing in the organisms (e.g. direct HCO_3^- uptake by the anion-exchange protein AE;

501   Drechsler and Beer 1991; Drechsler et al. 1993). But it's possible to assume that at least one common

502   or basal carbon concentrating mechanism (bCCM) is active. The most primitive mechanism is the

503   CO_2 diffusion (Cerling et al., 1993) that could be composed of two types of mitochondrial carbonic

504   anhydrase (e.g., internal and external) that enhance the fixation of Ci by recycling mitochondrial

505   CO_2 (Zabaleta et al., 2012). The role of carbonic anhydrase (CA) in algal photosynthesis was

506   described since the end-1960s (Bowes, 1969) and more recently detailed by Jensen et al. (2020),

507   who described the CA types and their functions. Also, the co-existence of different CCM's have

508   been described for the same specie (Axelsson et al., 1999, Xu et al., 2012), even that different CCM's

509   can operate simultaneously, generating different Ci contribution to RuBisCo internal pool

510   (Rautemberger et al., 2015). The variety of CCMs and their combinations contribute to the high $\delta^{13}C$

511   variability for the same species.

512   Because less carbon isotopic discrimination occurs when photosynthesis rates increases (Kübler and

513   Dungeon, 2015), less negative values in GCE macroalgae could evidence higher productivity in

514   subtropical seaweed communities than those in temperate marine ecosystems. Nevertheless, to

515   reflect high $\delta^{13}C$ on macroalgae tissue, they require saturating light intensity and enough nutrients

516   availability (Dudley et al., 2010), conditions occurring in the GCE waters. Based on the plant

517   communities' pattern, the macroalgal community productivity in GCE with intermediates values (so-

518   called 'hump-back'), belonging to intermediate productivity (Grime, 1970; Pärtel et al., 2007; Pärtel

519 and Zobel, 2007).

520 On the other hand, species that high efficiently HCO_3^- uptake, according to their $\delta^{13}C$ signal were to

521 35 (20%, >-10‰)) or 58 species (34%) of 170 species, if -11.5‰ (Δ of 1.5‰ as respiratory effect)

522 is the cutoff value for HCO_3^- users according to Carvalho and Eyre (2011). About 20-34% of species

523 could have the biochemical machinery to fix directly HCO_3^-, an efficient CCM that potencies the

524 productivity when is growing under optimal conditions. Furthermore, the highest $\delta^{13}C$ values have

525 been associated with the intermediate C3-C4 or C4 pathway (Valiela et al., 2018), which suggests

526 the presence of a more efficient CCM's than the typical C3 pathway. The C4 pathway reduces

527 photorespiration, the antagonist process of RuBisCo that cause a reduction in Ci assimilation about

528 25-40% (Ehleringer et al., 1991; Bauwe et al., 2010; Zabaleta et al., 2012). C4 pathway plants'

529 photorespiration reduction could be explained by their resource allocation, where they have more

530 investment in CCM than in RuBisCo protein content than plants with C3 pathway (Young et al.,

531 2016). Also, the reports of C4 or C4-like pathway in marine algae have increased in the last years

532 (Roberts et al., 2007; Doubnerová and Ryslavá, 2011; Xu et al.., 2012, 2013). High activity of keys

533 enzymes of C4 metabolism, such as pyruvate orthophosphate dikinase (PPDK),

534 phosphoenolpyruvate carboxylase (PEPC), and phosphoenolpyruvate carboxykinase (PCK), has

535 been described in macroalgae species. The establishment of a true C4 pathway in marine algae is not

536 clear since the massive changes in gene expression patterns seem to be no complete and it is

537 suggested that many marine algae have high plasticity to use a combination of CCM to overcome Ci

538 limitations (Roberts et al., 2007; Doubnerová and Ryslavá, 2011; Xu et al.., 2012, 2013). A Stepwise

539 model of the path from C3 to C4 photosynthesis is explained in Gowik and Westhoff (2011).

540 An elevated $\delta^{13}C$ signal in macroalgae can also be associated to calcifying species. For instance, in

541 our study, the genus *Amphiroa* and *Jania* both Rhodophyta with articulated-form, averaged -

542   7.86±3.7‰ and -9.37±0.75‰, respectively, which suggest the activity of a CCM using HCO_3^-

543   efficiently. Stepien (2015) reported a global mean of -14.83±1.0‰ for calcifying species compared

544   to -20.11±0.31‰ for non-calcifying species. High $\delta^{13}C$ values for calcifying species are related to

545   the excess of H^+ released as residuals products of the calcifying process, the acidified boundary

546   layers benefit the HCO_3^- uptake (McConnaughey & Whelan 1997, Courneau et a., 2012). In addition,

547   the high $\delta^{13}C$ values can be related to the highly efficient light properties enhanced in the carbonate

548   skeleton, resulting in an optimization of photosynthetic activity (Vasquez-Elizondo et al., 2016,

549   2017). Hofmann and Heesch (2018) reported high $\delta^{13}C$ values in eight rhodoliths species (calcifying

550   species) collected in deep habitats (25-40m) where light availability is low. High $\delta^{13}C$ has been

551   reported for other calcifying species (e.g., *Halimeda, Udotea, Penicillus* with $\delta^{13}C$ usually >10‰)

552   inhabiting seagrass meadows, where the light availability is limited by the *Thalassia testudinum*

553   canopy structure (Berger, 1981; Aharon, 1990; Oehlert et al., 2012; Enríquez et al., 2019). Another

554   case is *Padina* (frondose), a genus with lesser capacity to precipitate $CaCO_3$, but that show relatively

555   high $\delta^{13}C$ values (-12.49±2.48‰) (Ilus et al., 2017).

556   According to our fitted regression model to explain the variability of $\delta^{13}C$ by genera can be classified

557   from high (e.g. *Schizymenia* = -19.09‰), moderate (e.g. *Hydroclathrus* =7.33‰; *Amphiroa* =

558   6.84‰) and low variability (e.g. *Gracilaria* = -0.89; *Spyridia* = -1.46‰). Most species belong into

559   the moderate category, and these range of $\delta^{13}C$ values found is similar to those reported for algae

560   growing up between saturating (less negative values) or sub-saturating light intensity (more negative

561   values) (Hu et al., 2012; Rautemberger et al., 2015; Kübler and Dungeon, 2015). For instance,

562   experimental evidence by Rautemberger et al, (2015) showed *Ulva prolifera* growing under saturated

563   light at different pCO_2 levels showed the highest growth rates and activity of internal carbonic

564   anhydrase reached $\delta^{13}C$ signal >-10‰, higher than signal under low light regimen at same pCO_2

565   level. The authors concluded that CCM activity is energy and/or light dependent. Also, Kübler and

566   Dudgeon (2015) reported that pCO2 and temperature depend on the light intensities. Under sub-

567   saturating light intensities, pCO2 has a stronger effect on photosynthetic rates, and the temperature

568   effect increases at saturating light intensities. Light limitation effect on $\delta^{13}C$ signal has been observed

569   in deep subtidal habitats (Mercado et al., 2009; Hepburn et al., 2011; Marconi et al., 2011; Stepien

570   2015). Nevertheless, the depth in the shallow waters samples in our study was insufficient to find

571   significant differences in $\delta^{13}C$ between submareal and intertidal habitats. Even so, according to

572   multivariate linear regression analyses, the emersion level could explain a high percentage of the

573   variability be genus and morpho-functional groups.

574   Belonging to submareal habitats, we found three non-calcifying species (*Schizymenia pacifica,*

575   *Halymenia* sp., *Gigartina* sp.) of Rhodophyta with negatives values lesser than -30‰, which suggest

576   that are diffusive CO_2 users and for hence lack CCM. Their $\delta^{13}C$ signal are consistent with the results

577   of Murru and Sandgreen (2004) whose described *S. pacifica* and two species of *Halymenia* (e.g., *H.*

578   *schizymenioides* and *H. gardner*) as a restricted CO_2 user based on measurements of pH drift. Red

579   macroalgae that lack CCM, tend to inhabit in low-light habitats like subtidal or low intertidal and be

580   abundant in cold waters (Kübler et al., 1999, Raven et al., 2002a, Cornwall et al., 2015). According

581   to these authors, approximately 35% of the total red algae tested on a global scale are strictly CO_2

582   dependents. Our study evaluated 91 species of 453 red algae species reported in the Gulf of

583   California (Pedroche and Sentíes, 2003), which <3% of red macroalgae specimens could be Ci

584   limited. Low percentage of red macroalgae in the GCE lack of CCM, which can be partially

585   explained by the low solubility of CO_2 due to relatively high temperatures in subtropical waters

586   (Zeebe & Wolf-Gladrow, 2007). The percentage of macroalgae species representative of Arctic and

587   Antarctic ecosystems is 42-60% (Raven et al., 2002b; Iñiguez et al., 2019), 50% for temperate waters

588   of New Zealand (Hepburn et al., 2011) and until 90% found for a single site of Tazmania Australia

589   (Cornwall et al., 2015). In the GCE represents close 97%.

590   **Environment factors and δ^{13}C values**

591   We expect to found a difference in δ^{13}C values between eco-regions (e.g., north vs. south, peninsular

592   vs. continental), but non-geographical patterns were observed; neither differences associated to the

593   temperature for the same species o genus was observed. A slightly low δ^{13}C signal in communities

594   from C2 eco-region was observed, influenced by the Sonora desert.

595   Based on pH, differences in δ^{13}C were found only for a few genera (e.g. *Amphiroa, Colpomenia,*

596   *Ulva, Spyridia*), with a trend to increase in the δ^{13}C values with pH (Maberly et al., 1992, Raven et

597   al. 2002b). Similar results were reported for Cornwall et al. (2017) with differential response of the

598   δ^{13}C signals to pH among 19 species, in which only four species were sensitive to pH changes. Our

599   *in-situ* pH measurements do not represent the pH compensation point, the physiology measurement

600   indicates the presence or absence of CCM in photosynthetic organisms. Based on the complete

601   dataset, a weak but significant positive linear regression was observed between δ^{13}C and pH, similar

602   to the reported by Iñiguez et al. (2009) in three taxa of polar macroalgae. According to Stepien

603   (2015), the result of meta-analyzes between pH values and δ^{13}C was positive only for Rhodophyta

604   (R^2=0.41, p<0.001) and Ochrophyte (R^2=0.19, p<0.001), but not for Chlorophyta (R^2=0.002,

605   p<0.10). About 86% of the Stepien metadata met the theoretical CCM assignation based on both

606   parameters, exceptions for species with δ^{13}C<-30‰ that has been capable of raising pH>9.

607   Our lineal regression analyzes for latitudes showed a weak but significant correlation for the dataset

608   classified by for morphofunctional groups and genus, negative in the cases of Rhodophyta and

609   Ochrophyta groups (R^2=0.2 and 0.5, p<0.001), and a positive for Chlorophyta. The negative

610   correlation between latitude and δ^{13}C-algal was described by Stepien (2015), concluding that δ^{13}C

611   signal increased by 0.09‰ for each latitude degree from the Equator. Hofmann and Heesch (2018)

612   recently show a strong decrease in latitudinal effect (R^2= 0.43 δ^{13}C$_{total}$ and 0.13, for δ^{13}C$_{organic-tissue}$,

613   p=0.001) for rhodoliths of the northern hemisphere and macroalgae from coral reefs in Australia. In

614   both cases, the latitude range is higher than we tested (30º to 80º and from 10º to 45º, respectively).

615   These differences on a big scale tend to be associated with a temperature effect (Stepien, 2015) and

616   their effect on CO2 solubility in S.W. (Zeebe & Wolf-Gladrow, 2007). Even so, our multivariate

617   linear regression analyses showed that the environmental factors were significant (p=0.001),

618   explaining up to 50% of the δ^{13}C variability.

619   **Morphofunctional groups and δ^{13}C**

620   The variability recorded on morphofunctional groups was high, mostly influenced by the genus. The

621   highest δ^{13}C values were found in R-larger size articulated y R-smaller-side articulated composed

622   by *Amphiroa* and *Jania* spp, respectively, also O-hollow with spherical composed by *Colpomenia*

623   spp. Based on the literature, Stepien (2015) made an analyze about morphofunctional groups and

624   δ^{13}C by following the group proposed by Littler & Littler (1980) and modified by Balata et al., (2012)

625   and they agreed that morphofunctional groups that are composed by calcifying species (e.g. crust

626   calcifiers) have highest δ^{13}C signal. Our regression models showed that morphofunctional groups

627   have a R^2 adjusted =0.34, and increase to genus (R^2 adjusted =0.41,) and to species (R^2 adjusted

628   =0.46). This result is consistent with reported by Lovelock et al., (2020), which found that 66% of

629   δ^{13}C variability was explained by taxonomy. Although morphofunctional groups could explain less

630   than genus or species, it is a great tool to increase the possibility of analyzes on a big spatial scale,

631   especially when the species distribution could be limited.

632

Conclusions

634 Our work confirms that taxonomy is the main cause of $\delta^{13}C$ variability among seaweed communities

635 analyzed and explained until 46%. Most species showed a $\delta^{13}C$ belong into a range that indicates a

636 mix of CO_2 and HCO_3^- uptake. About 20-34% species depending on cutoff limits for CCM presence

637 showed at least one specimen with $\delta^{13}C$>-10‰, suggesting that potentially could have highly

638 efficient CCM. On the other extreme, some Rhodophyta species relied exclusively on diffusive CO_2

639 entry, as inferred from their $\delta^{13}C$ values (i.e. $\delta^{13}C$ lower than -30‰; *Schizymenia pacifica,*

640 *Halymenia* sp., and *Gigartina* sp.). Even so, $\delta^{13}C$ variability associated with species can be classified

641 in high (-19‰), moderate (7‰), low (0.89‰). This variability range is similar to $\delta^{13}C$ values

642 between growing under saturating light (high values) and no saturating (low values). Specimens

643 collected from the subtidal habitat showed more negative $\delta^{13}C$ values (higher discrimination) than

644 the intertidal habitat, but without significant difference. The percent of Rhodophyta species (3.26%)

645 that could be Ci limited (without evident CCM activity) is relatively low in comparison that reported

646 for temperate regions (40-90%). The data presented indicate that HCO_3^- uptake by active transport

647 is widespread among GC algae. In this sense, $\delta^{13}C$ provide information about the physiological and

648 environmental status of macroalgae.

649

6. References

Abbot, I. A., & Hollenberg, G. (1976). Marine algae of California. Standford University Press, California.

Aguilar-Rosas, L. E., & R. Aguilar-Rosas, 1993. Ficogeografía de las algas pardas (Phaeophyta) de la península de Baja California. In S. I. Salazar-Vallejo y N. E. González (eds.), Biodiversidad Marina y Costera de México (pp. 197–206). Comisión Nacional Biodiversidad y CIQRO, México.

Aharon, P. (1991). Recorders of reef environment histories: stable isotopes in corals, giant clams, and calcareous algae. *Coral Reefs*, 10(2), 71–90. https://doi.org/10.1007/BF00571826

Álvarez-Borrego, S. (1983). Gulf of California. In: Ketchum BH (ed.), Ecosystems of the World, 26. *Estuaries and Enclosed Seas,* (pp. 427–449). Elsevier, Amsterdam.

Axelsson, L., Ryberg, H., & Beer, S. (1995). Two modes of bicarbonate utilization in the marine green macroalga *Ulva lactuca. Plat cell & environment,* 18, 439–445. https://doi.org/10.1111/j.1365-3040.1995.tb00378.x

Axelsson, L., Larsson, C., & Ryberg, H. (1999). Affinity, capacity and oxygen sensitivity of two different mechanisms for bicarbonate utilization in *Ulva lactuca* L. (Chlorophyta). *Plat cell & environment*, 22, 969–978. https://doi.org/10.1046/j.1365-3040.1999.00470.x

Balata, D., Piazzi, L., & Rindi, F. (2011). Testing a new classification of morphological functional groups of marine macroalgae for the detection of responses to stress. *Marine Biology*, 158, 2459–69. https://doi.org/10.1007/s00227-011-1747-y

Bastidas-Salamanca, M., Gonzalez-Silvera, A., Millán-Núñez, R., Santamaria-del-Angel, E., & Frouin, R. (2014). Bio-optical characteristics of the Northern Gulf of California during June 2008. *International Journal of Oceanography*, 2014. https://doi.org/10.1155/2014/384618

Bauwe, H., Hagemann, M., & Fernie, A. R. (2010). Photorespiration: players, partners and origin. *Trends in plant science*, 15(6), 330–336. https://doi.org/10.1016/j.tplants.2010.03.006

Beardall, J., & Giordano, M. (2002). Ecological implications of microalgal and cyanobacterial CO_2 concentrating mechanisms, and their regulation. *Functional Plant Biology*, 29(3), 335–347.

680 https://doi.org/10.1071/PP01195

681 Bold, C. H., & Wynne, J. M. (1978). Introduction to the Algae. Structure and reproduction. Prentice-
682 Hall, Incorporated.

683 Bowes, G. W. (1969). Carbonic anhydrase in marine algae. *Plant Physiology,* 44:726–732.
684 https://doi.org/10.1104/pp.44.5.726

685 Bray, N. A. (1988). Thermohaline circulation in the Gulf of California. *Journal of Geophysical*
686 *Research*: *Oceans*, 93(C5), 4993–5020. https://doi.org/10.1029/JC093iC05p04993

687 Burnham, K. P., & Anderson, D. R. (2002). A practical information-theoretic approach. Model
688 selection and multimodel inference, 2nd ed. Springer, New York, 2.

689 Carrillo, L., & Palacios-Hernández, E. (2002). Seasonal evolution of the geostrophic circulation in
690 the northern Gulf of California. *Estuarine, Coastal and Shelf Science*, 54(2), 157–173.
691 https://doi.org/10.1006/ecss.2001.0845

692 Carvalho, M. C. & Eyre, B. D. (2011). Carbon stable isotope discrimination during respiration in
693 three seaweed species. *Marine Ecology Progress Series*, 437:41–49.
694 https://doi.org/10.3354/meps09300

695 Cerling, T. E., Wang, Y., & Quade, J. (1993). Expansion of C4 ecosystems as an indicator of global
696 ecological change in the late Miocene. *Nature*, 361 (6410), 344–345.
697 https://doi.org/10.1038/361344a0

698 Comeau, S., Carpenter, R. C., & Edmunds, P. J. (2012). Coral reef calcifiers buffer their response to
699 ocean acidification using both bicarbonate and carbonate. *Proceedings of the Royal Society B:*
700 *Biological Sciences*, 280(1753), 20122374. https://doi.org/10.1098/rspb.2012.2374

701 CNA (Comisión Nacional del Agua). (2012). Atlas del agua en México.

702 Cornwall, C. E., Revill, A.T., & Hurd, C. L. (2015). High prevalence of diffusive uptake of CO_2 by
703 macroalgae in a temperate subtidal ecosystem. *Photosynthesis Research*, 124, 181–190.
704 https://doi.org/10.1007/s11120-015-0114-0

705 Cornwall, C. E., Revill, A. T., Hall-Spencer, J. M., Milazzo, M., Raven, J. A., & Hurd, C. L. (2017).

706   Inorganic carbon physiology underpins macroalgal responses to elevated CO_2. *Scientific Reports*,

707   7(1), 1–12. https://doi.org/10.1038/srep46297

708   Dawson, E. Y. (1944). The marine algae of the Gulf of California. *Allan Hancock Pacific*

709   *Expeditions*, 3(10), [i-v+] 189–453.

710   Dawson, E. Y. (1954). Marine red algae of Pacific México. Part 2. *Cryptonemiales* (cont.). *Allan*

711   *Hancock Pacific Expeditions,* 17(2), 241–397.

712   Dawson, E. Y. (1956). How to know the seaweeds. Dubuque, Iowa, USA. W.M.C. Brown. Co.

713   Publishers. pp 197.

714   Dawson, E. Y. (1961). Marine red algae of Pacific México. Part 4. *Gigartinales*. *Pacific Naturalist*.

715   2, 191–343.

716   Dawson, E. Y. (1962). Marine red algae of Pacific México. Part 7. *Ceramiales*: Ceramiciaceae,

717   Delesseriaceae. *Allan Hancock Pacific Expeditions*, 26(1), 1–207.

718   Dawson, E. Y. (1963). Marine red algae of Pacific México. Part 8. *Ceramiales*: Dasyaceae,

719   Rhodomelaceae. Nova Hedwigia. 5, 437–476.

720   Doubnerová, V., & Ryšlavá, H. (2011). What can enzymes of C4 photosynthesis do for C3 plants

721   under stress?. *Plant Science*, 180(4), 575–583. https://doi.org/10.1016/j.plantsci.2010.12.005

722   Draper, N. R., & Smith, H. (1998). Applied regression analysis (Vol. 326). John Wiley & Sons.

723   Drechsler, Z., & Beer, S. (1991). Utilization of inorganic carbon by *Ulva lactuca*. *Plant Physiology,*

724   97, 1439–1444. https://doi.org/10.1104/pp.97.4.1439

725   Drechsler, Z., Sharkia, R., Cabantchik, Z. I., & Beer, S. (1993). Bicarbonate uptake in the marine

726   macroalga *Ulva* sp. is inhibited by classical probes of anion exchange by red blood cells. *Planta*,

727   191(1), 34–40. https://doi.org/10.1007/BF00240893

728   Dudgeon, S. R., Davison, I. R., & Vadas, R. L. (1990). Freezing tolerance in the intertidal red algae

729   *Chondrus crispus* and *Mastocarpus stellatus:* Relative importance of acclimation and adaptation.

730   *Marine Biology*, 106(3), 427–436. https://doi.org/10.1007/BF01344323

731   Dudley, B. D., Barr, N. G., & Shima, J. S. (2010). Influence of light intensity and nutrient source on

732 δ^{13}C and δ^{15}N signatures in *Ulva pertusa. Aquatic Biology*, 9(1), 85–93.

733 https://doi.org/10.3354/AB00241

734 Ehleringer, J. R., Cerling, T. E., & Helliker, B. R. (1997). C4 photosynthesis, atmospheric CO_2, and

735 climate. *Oecologia*, 112(3), 285–299. https://doi.org/10.1007/s004420050311

736 Ehleringer, J. R., Sage, R. F., Flanagan, L. B., & Pearcy, R. W. (1991). Climate change and the

737 evolution of C4 photosynthesis. *Trends in ecology & evolution*, 6(3), 95–99.

738 https://doi.org/10.1073/pnas.1718988115

739 Enríquez, S., Agustí, S. & Duarte, C. (1994). Light absorption by marine macrophytes. *Oecologia*.

740 98:121–129. https://doi.org/10.1007/BF00341462

741 Enriquez, S., & Sand-Jensen, K. (2003). Variation in light absorption properties of *Mentha aquatica*

742 L. as a function of leaf form: implications for plant growth. *International journal of plant sciences*,

743 164(1), 125–136. https://doi.org/10.1086/344759

744 Enríquez, S., & Rodríguez-Román, A. (2006). Effect of water flow on the photosynthesis of three

745 marine macrophytes from a fringing-reef lagoon. *Marine Ecology Progress Series*, 323, 119–132.

746 https://doi.org/10.3354/meps323119

747 Enríquez, S., Olivé, I., Cayabyab, N., & Hedley, J. D. (2019). Structural complexity governs seagrass

748 acclimatization to depth with relevant consequences for meadow production, macrophyte diversity

749 and habitat carbon storage capacity. *Scientific reports*, 9(1), 1–14. https://doi.org/10.1038/s41598-

750 019-51248-z

751 Espinoza-Avalos, J. (1993). Macroalgas marinas del Golfo de California. *In*: SI Salazar-Vallejo, NE

752 González (eds.), *Biodiversidad marina y costera de México*. CONABIO- CIQRO, México. 328–357.

753 Espinosa-Carreón, T. L., & Valdez-Holguín, E. (2007). Variabilidad interanual de clorofila en el

754 Golfo de California. *Ecología aplicada*, 6(1-2), 83–92.

755 Espinosa-Carreón, T. L., & Escobedo-Urías, D. (2017). South region of the Gulf of California large

756 marine ecosystem upwelling, fluxes of CO_2 and nutrients. *Environmental development*, 22, 42–51.

757 https://doi.org/10.1016/j.envdev.2017.03.005

758   Fernández, P. A., Hurd, C. L., & Roleda, M. Y. (2014). Bicarbonate uptake via an anion exchange

759   protein is the main mechanism of inorganic carbon acquisition by the giant kelp *Macrocystis pyrifera*

760   (Laminariales, Phaeophyceae) under variable pH. *Journal of phycology*, 50(6), 998–1008.

761   https://doi.org/10.1111/jpy.12247

762   Fernández, P. A., Roleda, M. Y., & Hurd, C. L. (2015). Effects of ocean acidification on the

763   photosynthetic performance, carbonic anhydrase activity and growth of the giant kelp *Macrocystis*

764   *pyrifera*. *Photosynthesis Research*, 124(3), 293–304. https://doi.org/10.1007/s11120-015-0138-5

765   Gateau, H., Solymosi, K., Marchand, J., & Schoefs, B. (2017). Carotenoids of microalgae used in

766   food industry and medicine. Mini reviews in medicinal chemistry, 17(13), 1140–1172.

767   https://doi.org/10.2174/1389557516666160808123841

768   Gilbert, J. Y., & Allen, W. E. (1943). The phytoplankton of the Gulf of California obtained by the

769   ''E.W. Scripps'' in 1939 and 1940. *Journal of Marine Research*, 5, 89–110.

770   https://doi.org/10.1016/0022-0981(67)90008-1

771   Giordano, M., Beardall, J., & Raven, J. A. (2005). CO_2 concentrating mechanisms in algae:

772   mechanisms, environmental modulation and evolution. *Annual Review of Plant Biology,* 66:99–131.

773   https://doi.org/10.1146/annurev.arplant.56.032604.144052

774   Gowik, U., & Westhoff, P. (2012). The path from C3 to C4 photosynthesis. *Plant Physiology*, 155(1),

775   56–63. https://doi.org/10.1104/pp.110.165308

776   Grime, J. P. (1977). Evidence for the existence of three primary strategies in plants and its relevance

777   to ecological and evolutionary theory. *The American Naturalist*, 111(982), 1169–1194.

778   Hepburn, C. D., Pritchard, D. W., Cornwall, C. E., McLeod, R.J., Beardall, J., Raven, J. A., & Hurd,

779   C. L. (2011). Diversity of carbon use strategies in a kelp forest community: implications for a high

780   CO_2 ocean. *Global Change Biology*, 17, 2488–2497. https://doi.org/10.1111/j.1365-

781   2486.2011.02411.x.

782   Hofmann, L., & Heesch, S. (2018). Latitudinal trends in stable isotope signatures and carbon-

783   concentrating mechanisms of northeast Atlantic rhodoliths. *Biogeosciences*, 15, 6139–6149.

784   https://doi.org/10.5194/bg-15-6139-2018

785   Hopkinson, B.M., Dupont, C.L., Allen, A.E., & Morel, F.M.M. (2011). Efficiency of the CO_2-

786   concentrating mechanism of diatoms. Proceedings of the National Academy of Sciences of the

787   United States of America, 108, 3830–3837. https://doi.org/10.1073/pnas.1018062108

788   Hopkinson, B.M., Young, J.N., Tansik, A.L., & Binder, B.J. (2014). The minimal CO_2 concentrating

789   mechanism of *Prochlorococcus* MED4 is effective and efficient. *Plant Physiology*, 166, 2205–2217.

790   https://doi.org/10.1104/pp.114.247049

791   Hu, X., Burdige, D. J., & Zimmerman, R. C. (2012). $\delta^{13}C$ is a signature of light availability and

792   photosynthesis in seagrass. *Limnology and oceanography*, 57(2), 441–448.

793   https://doi.org/10.4319/lo.2012.57.2.0441

794   Hurd, C.L. (2000). Water motion, marine macroalgal physiology, and production. *Journal of*

795   *Phycology*, 36, 453–472. https://doi.org/10.1046/j.1529-8817.2000.99139.x

796   Iluz, D., Fermani, S., Ramot, M., Reggi, M., Caroselli, E., Prada, F., et al. (2017). Calcifying

797   response and recovery potential of the brown alga *Padina pavonica* under ocean acidification. *ACS*

798   *Earth and Space Chemistry*, 1(6), 316–323. https://doi.org/10.1021/acsearthspacechem.7b00051

799   Iñiguez, C., Galmés, J., & Gordillo, F. J. (2019). Rubisco carboxylation kinetics and inorganic

800   carbon utilization in polar versus cold-temperate seaweeds. *Journal of experimental botany*, 70(4),

801   1283–1297. https://doi.org/10.1093/jxb/ery443

802   Jensen, E. L., Maberly, S. C., & Gontero, B. (2020). Insights on the functions and ecophysiological

803   relevance of the diverse carbonic anhydrases in microalgae. *International Journal of Molecular*

804   *Sciences,* 21(8), 2922. https://doi.org/10.3390/ijms21082922

805   Kim, M. S., Lee, S. M., Kim, H. J., Lee, S. Y., Yoon, S. H., & Shin, K. H. (2014). Carbon stable

806   isotope ratios of new leaves of *Zostera marina* in the mid-latitude region: implications of seasonal

807   variation in productivity. *Journal of experimental marine biology and ecology,* 461, 286–296.

808   https://doi.org/10.1016/j.jembe.2014.08.015

809   Kirk, J. T. O. (2011). Light and Photosynthesis in Aquatic Ecosystems. 3rd ed. Cambridge University

810   Press, Cambridge.

811   Klenell, M., Snoeijs, P., & Pedersen, M. (2004). Active carbon uptake in *Laminaria digitata* and *L.*

812   *saccharina* (Phaeophyta) is driven by a proton pump in the plasma membrane. *Hydrobiologia,* 514,

813   41–53. https://doi.org/10.1023/B:hydr.0000018205.80186.3e

814   Kremer, B. P. (1981). Metabolic implications of non-photosynthetic carbon fixation in brown

815   macroalgae. *Phycologia*, 20(3), 242–250. https://doi.org/10.2216/i0031-8884-20-3-242.1

816   Kübler, J. E., & Davison, I. R. (1993). High-temperature tolerance of photosynthesis in the red alga

817   *Chondrus crispus.* Marine Biology, 117(2), 327–335. https://doi.org/10.1007/BF00345678

818   Kübler, J., Johnston, E., Andrew, M., & Raven, J. A. (1999). The effects of reduced and elevated

819   CO_2 and O_2 on the seaweed *Lomentaria articulata*. *Plat cell & environment,* 22, 1303–1310.

820   https://doi.org/10.1046/j.1365-3040.1999.00492.x

821   Kübler, J. E., & Dudgeon, S. R. (2015). Predicting effects of ocean acidification and warming on

822   algae   lacking   carbon   concentrating   mechanisms.   *PLoS   One,*   10   (7).

823   https://doi.org/10.1371/journal.pone.0132806

824   Küppers, U., & Kremer, B. P. (1978). Longitudinal profiles of carbon dioxide fixation capacities in

825   marine macroalgae. *Plant Physiology*, 62(1), 49–53. https://doi.org/10.1104/pp.62.1.49

826   Kustka, A. B., Milligan, A. J., Zheng, H., New, A. M., Gates, C., Bidle, K. D., & Reinfelder, J. R.

827   (2014). Low CO_2 results in a rearrangement of carbon metabolism to support C4 photosynthetic

828   carbon   assimilation   in   *Thalassiosira   pseudonana*.   *New   Phytologist*,   204(3),   507–520.

829   https://doi.org/10.1111/nph.12926

830   Lapointe, B. E., & Duke, C. S. (1984). Biochemical strategies for growth of *Gracilaria tikvahiae*

831   (Rhodophyta) in relation to light intensity and nitrogen availability. *Journal of Phycology*, 20(4),

832   488–495. https://doi.org/10.1111/j.0022-3646.1984.00488.x

833   Littler, M. M., & Littler, D. S. (1980). The evolution of thallus form and survival strategies

834   in benthic marine macroalgae: field and laboratory tests of a functional form model. *The*

835   *American Naturalist*, 116, 25–44.

836

837 Littler, M. M., & Arnold, K. E. (1982). Primary productivity of marine macroalgal

838 functional-form groups from south-western North America. *Journal of Phycology*, 18, 307–

839 311. https://doi.org/10.1111/j.1529-8817.1982.tb03188.x

840

841 Littler, M.M., & Littler, D.S., (1984). Relationships between macroalgal functional form

842 groups and substrata stability in subtropical rocky intertidal system. *Journal of Experimental*

843 *Marine Biolology and Ecology*, 74, 13–34. https://doi.org/10.1016/0022-0981(84)90035-2

844

845 Lovelock, C. E., Reef, R., Raven, J. A., & Pandolfi, J. M. (2020). Regional variation in δ^{13}C

846 of coral reef macroalgae. *Limnology and Oceanography*. https://doi.org/10.1002/lno.11453

847

848 Lluch-Cota, S. E., Aragón-Noriega, E. A., Arreguín-Sánchez, F., Aurioles-Gamboa, D., Bautista-

849 Romero, J. J., Brusca, R. C, et al. (2007). The Gulf of California: Review of ecosystem status and

850 sustainability challenges. *Progress in Oceanography,* 73, 1–26.

851 https://doi.org/10.1016/j.pocean.2007.01.013

852 Maberly, S. C., Raven, J. A. & Johnston, A. M. (1992). Discrimination between ^{12}C and ^{13}C by

853 marine plants. *Oecologia,* 91,481–492. https://doi.org/10.1007/BF00650320

854 Madsen, T. V., & Maberly, S. C. (2003). High internal resistance to CO_2 uptake by submerged

855 macrophytes that use HCO_3^- : measurements in air, nitrogen and helium. *Photosynthesis research*,

856 77(2-3), 183–190. https://doi.org/10.1023/A:1025813515956

857 Marinone, S. G., & Lavín, M. F. (2003). Residual flow and mixing in the large islands' region of the

858 central Gulf of California. In Nonlinear processes in geophysical fluid dynamics (pp. 213–236).

859 Springer, Dordrech. http://doi-org-443.webvpn.fjmu.edu.cn/10.1007/978-94-010-0074-1_13

860 Marinone, S.G. (2007). A note on "Why does the Ballenas Channel have the coldest SST in the Gulf

861 of California?". *Geophysical research letters*, 34(2). https://doi.org/10.1029/2006GL028589

862 Marconi, M., Giordano, M, & Raven, J.A. (2011). Impact of taxonomy, geography and depth on the

863 δ^{13}C and δ^{15}N variation in a large collection of macroalgae. *Journal of Phycology,* 47, 1023–1035.

864 https://doi.org/10.1111/j.1529-8817.2011.01045.x

865   Marshall, J. D., Brooks, J. R., & Lajtha, K. (2007). Sources of variation in the stable isotopic

866   composition of plants. Stable isotopes in ecology and environmental science, 2, 22–60.

867   https://doi.org/10.1002/9780470691854.ch2

868   Martínez-Díaz-de-León, A. (2001). Upper-ocean circulation patterns in the Northern Gulf of

869   California, expressed in Ers-2 synthetic aperture radar imagery. *Ciencias Marinas*, 27(2), 209–221.

870   https://doi.org/10.7773/cm.v27i2.465

871   Martínez-Díaz-de-León, A., Pacheco-Ruíz, I., Delgadillo-Hinojosa, F., Zertuche-González, J. A.,

872   Chee-Barragán, A., Blanco-Betancourt, R., et al. (2006). Spatial and temporal variability of the sea

873   surface temperature in the Ballenas-Salsipuedes Channel (central Gulf of California). *Journal of*

874   *Geophysical Research: Oceans,* 111(C2). https://doi.org/10.1029/2005JC002940

875   Masojidek, J., Kopecká, J., Koblížek, M., & Torzillo, G. (2004). The xanthophyll cycle in green

876   algae (Chlorophyta): its role in the photosynthetic apparatus. *Plant Biology*, 6(3), 342–349.

877   https://doi.org/10.1055/s-2004-820884

878   McConnaughey, T. A., Burdett, J., Whelan, J. F., & Paull, C. K. (1997). Carbon isotopes in biological

879   carbonates: respiration and photosynthesis. *Geochimica et Cosmochimica Acta*, 61(3), 611–622.

880   https://doi.org/10.1016/S0016-7037(96)00361-4

881   Mercado, J. M., De los Santos, C. B., Pérez-Lloréns, J. L., & Vergara, J. J. (2009). Carbon isotopic

882   fractionation in macroalgae from Cadiz Bay (Southern Spain): comparison with other bio-

883   geographic regions. *Estuarine, Coastal and Shelf Science,* 85, 449–458.

884   https://doi.org/10.1016/j.ecss.2009.09.005

885   Murru, M. & Sandgren, C. D. (2004). Habitat matters for inorganic carbon acquisition in 38 species

886   of red macroalgae (Rhodophyta) from Puget Sound, Washington, USA. *Journal of Phycology,* 40,

887   837–845. https://doi.org/10.1111/j.1529-8817.2004.03182.x

888   Nielsen, S. L., & Jensen, K. S. (1990). Allometric settling of maximal photosynthetic growth rate to

889   surface/volume ratio. *Limnology and Oceanography*, 35(1), 177–180.

890   https://doi.org/10.4319/lo.1990.35.1.0177

891   Norris, J. N. (2010). Marine algae of the northern Gulf of California: Chlorophyta and Phaoephyceae.

892   Series: *Smithsonian contributions to Botany*, no. 94. https://doi.org/10.5479/si.19382812.96

893   Oehlert, A. M., Lamb-Wozniak, K. A., Devlin, Q. B., Mackenzie, G. J., Reijmer, J. J., &
894   Swart, P. K. (2012). The stable carbon isotopic composition of organic material in platform
895   derived sediments: implications for reconstructing the global carbon cycle. *Sedimentology*,
896   59(1), 319–335. https://doi.org/10.1111/j.1365-3091.2011.01273.x
897

898   Ochoa-Izaguirre, M. J., Aguilar-Rosas, R., & Aguilar-Rosas, L. E. (2007). Catálogo de Macroalgas
899   de las lagunas costeras de Sinaloa. Serie Lagunas Costeras. Páez-Osuna, F. (Ed.). UNAM, ICMyL,
900   México, pp 117.

901   Ochoa-Izaguirre, M. J., & Soto-Jiménez, M. F. (2015). Variability in nitrogen stable isotope
902   ratios of macroalgae: consequences for the identification of nitrogen sources. *Journal of
903   Phycology*, 51, 46–65. https://doi.org/10.1111/jpy.12250
904

905   O'Leary, M. H. (1988). Carbon isotopes in photosynthesis. *Bioscience*, *38*(5), 328–336.
906   https://doi.org/10.2307/1310735
907

908   O'Leary, M. H. (1993). Biochemical basis of carbon isotope fractionation. In *Stable isotopes
909   and   plant   carbon-water   relations* (pp.   19–28).   Academic   Press.
910   https://doi.org/10.1016/B978-0-08-091801-3.50009-X
911

912   Páez-Osuna, F., Sánchez-Cabeza, J. A., Ruiz-Fernández, A. C., Alonso-Rodríguez, R.,
913   Piñón-Gimate, A., Cardoso-Mohedano, J. G., et al. (2017). Environmental status of the Gulf
914   of   California: a   pollution   review. *Earth-Science   Reviews*,   166,   181–205.
915   https://doi.org/10.1016/j.earscirev.2016.09.015
916

917   Pärtel, M., Laanisto, L., & Zobel, M. (2007). Contrasting plant productivity–diversity
918   relationships across latitude: the role of evolutionary history. *Ecology*, 88(5), 1091–1097.
919   https://doi.org/10.1890/06-0997
920

921 Pärtel, M., & Zobel, M. (2007). Dispersal limitation may result in the unimodal productivity-
922 diversity relationship: a new explanation for a general pattern. *Journal of Ecology*, 95(1), 90–
923 94. https://doi.org/10.1111/j.1365-2745.2006.01185.x

924

925 Pedroche, F. F., & Sentíes, A. (2003). Ficología marina mexicana: Diversidad y Problemática
926 actual. *Hidrobiológica*, 13(1), 23–32.

927

928 Rautenberger, R., Fernandez, P. A., Strittmatter, M., Heesch, S., Cornwall, C. E., Hurd, C. L., &
929 Roleda, M. Y. (2015). Saturating light and not increased carbon dioxide under ocean acidification
930 drive photosynthesis and growth in *Ulva rigida* (Chlorophyta). *Ecology and evolution*, 5(4), 874–
931 888. https://doi.org/10.1002/ece3.1382

932 Raven, J. A., Johnston, A. M., Kübler, J. E., Korb, R. E., McInroy, S. G., Handley, L. L., et al.
933 (2002a). Seaweeds in cold seas: evolution and carbon acquisition. *Annals of Botany,* 90, 525–536.
934 https://doi.org/10.1093/aob/mcf171

935 Raven, J. A., Johnshton, A. M., Kübler, J. E., Korb, R. E., Mclnroy, S. G., Handley, L. L., et al.
936 (2002b). Mechanistic interpretation of carbon isotope discrimination by marine macroalgae and
937 seagrasses. *Functional Plant Biology,* 29:355–378. https://doi.org/10.1071/PP01201

938 Raven, J. A., Ball, L. A., Beardall, J., Giordano, M., & Maberly, S. C. (2005). Algae lacking carbon-
939 concentrating mechanisms. *Canadian Journal of Botany*, 83(7), 879–890.
940 https://doi.org/10.1139/b05-074

941 Raven, J. A., & Hurd, C. (2012). Ecophysiology of photosynthesis in macroalgae. *Photosynthesis*
942 *Research,* 113, 105–125. https://doi.org/10.1007/s11120-012-9768-z

943 Raven, J. A., & Beardall, J. (2016). The ins and outs of CO_2. *Journal of Experimental*
944 *Botany*, *67*(1), 1–13. https://doi.org/10.1093/jxb/erv451

945

946 Reiskind, J. B., Seamon, P. T., & Bowes, G. (1988). Alternative methods of photosynthetic carbon
947 assimilation in marine macroalgae. *Plant Physiology,* 87, 686–692.
948 https://doi.org/10.1104/pp.87.3.686

949   Reiskind, J. B., & Bowes, G. (1991). The role of phosphoenolpyruvate carboxykinase in a marine

950   macroalga with C4-like photosynthetic characteristics. *Procceding of the National Academy of*

951   *Science of the United States of America*, 88, 2883–2887. https://doi.org/10.1073/pnas.88.7.2883

952   Roberts, K., Granum, E., Leegood, R. C., & Raven, J. A. (2007). C3 and C4 pathways of

953   photosynthetic carbon assimilation in marine diatoms are under genetic, not environmental, control.

954   *Plant physiology*, 145(1), 230–235. https://doi.org/10.1104/pp.107.102616

955   Roden, G.I., & Groves, G.W. (1959). Recent oceanographic investigations in the Gulf of California.

956   *Journal of Marine Research*, 18(1), 10–35.

957   Roden, G.I., & Emilsson, L. (1979). Physical oceanography of the Gulf of California. Simposium

958   Golfo de California, Universidad Nacional Autónoma de México, Mazatlán, Sinaloa, México.

959   Rusnak, G.A., Fisher, R. L., & Shepard, F.P. (1964). Bathymetry and faults of Gulf of California.

960   In: van Andel, Tj. H. and G.G. Shor, Jr. (editors). Marine Geology of the Gulf of California: A

961   symposium. *The American Association of Petroleum Geologists, Memoir*, 3, 59–75.

962   https://doi.org/10.1306/M3359C3

963   Santamaría-del-Angel, E., Alvarez-Borrego, S., & Müller-Karger, F.E. (1994). Gulf of

964   California biogeographic regions based on coastal zone color scanner imagery. *Journal of*

965   *Geophysical Research*, 99, 7411–7421. https://doi.org/10.1029/93JC02154

966

967   Sanford, L.P., & Crawford, S.M. (2000). Mass transfer versus kinetic control of uptake across solid-

968   water boundaries. *Limnology and Oceanography*, 45, 1180−1186.

969   https://doi.org/10.4319/lo.2000.45.5.1180

970   Sand-Jensen, K., & Gordon, D. (1984). Differential ability of marine and freshwater macrophytes to

971   utilize HCO_3^- and CO_2. *Marine Biology,* 80, 247–253. https://doi.org/10.1111/j.1469-

972   8137.1981.tb03198.x

973   Setchell, W., & Gardner, N. (1920). The marine algae of the Pacific Coast of North America. Part II

974   Chlorophyceae. *University of California: Publications in Botany,* 8, 139–374.

975   https://doi.org/10.5962/bhl.title.5719

976

977   Setchell, W., & Gardner, N. (1924). The marine algae. *In* Expedition of the California Academy of

978   Sciences to the Gulf of California in 1921. *Proceedings of the California Academy of Sciences, 4th*

979   *series,* 12(29), 695–949.

980   Sharkey, T. D., & Berry, J. A. (1985). Carbon isotope fractionation of algae as influenced by an

981   inducible CO_2 concentrating mechanism. Inorganic carbon uptake by aquatic photosynthetic

982   organisms (pp. 389–401).

983   Stepien, C. C. (2015). Impacts of geography, taxonomy and functional group on inorganic carbon

984   use patterns in marine macrophytes. *Journal of Ecology*, 103(6), 1372–1383.

985   https://doi.org/10.1111/1365-2745.12451

986   Stepien, C. C., Pfister, C. A., & Wootton, J. T. (2016). Functional traits for carbon access in

987   macrophytes. *PloS one,* 11(7), e0159062. https://doi.org/10.1371/journal.pone.0159062

988   Valiela, I., Liu, D., Lloret, J., Chenoweth, K., & Hanacek, D. (2018). Stable isotopic evidence

989   of nitrogen sources and C4 metabolism driving the world's largest macroalgal green tides in

990   the Yellow Sea. *Scientific reports*, 8(1), 1–12. https://doi.org/10.1038/s41598-018-35309-3

991

992   Vásquez-Elizondo, R. M., Legaria-Moreno,· Pérez-Castro, M.A., Krämer, W. E., · Scheufen, T.,

993   Iglesias-Prieto, R., & Enríquez, S. (2017). Absorptance determinations on multicellular tissues.

994   *Photosynthesis Research*, 132, 311–324. https://doi.org/10.1007/s11120-017-0395-6

995   Vásquez-Elizondo, R. M., & Enríquez, S. (2017). Light absorption in coralline algae (Rhodophyta):

996   a morphological and functional approach to understanding species distribution in a coral reef lagoon.

997   *Frontiers in Marine Science*, 4, 297. https://doi.org/10.3389/fmars.2017.00297

998   Velasco-Fuentes, O. V., & Marinone, S. G. (1999). A numerical study of the Lagrangian circulation

999   in the Gulf of California. *Journal of Marine Systems*, 22(1), 1–12. https://doi.org/10.1016/S0924-

1000   7963(98)00097-9

1001   Young, E. B., & Beardall, J. (2005). Modulation of photosynthesis and inorganic carbon acquisition

1002   in a marine microalga by nitrogen, iron, and light availability. *Canadian Journal of Botany*, 83(7),

1003   917–928. https://doi.org/10.1139/b05-081

1004 Young, J. N., Heureux, A. M., Sharwood, R. E., Rickaby, R. E., Morel, F. M., & Whitney, S. M.
1005 (2016). Large variation in the Rubisco kinetics of diatoms reveals diversity among their carbon-
1006 concentrating mechanisms. *Journal of Experimental Botany*, 67(11), 3445–3456.
1007 https://doi.org/10.1093/jxb/erw163

1008 Xu, J., Fan, X., Zhang, X., Xu, D., Mou, S., Cao, S., et al. (2012). Evidence of coexistence of C3
1009 and C4 photosynthetic pathways in a green-tide-forming alga, *Ulva prolifera. PloS one*, 7(5),
1010 e37438. https://doi.org/10.1371/journal.pone.0037438

1011 Xu, J., Zhang, X., Ye, N., Zheng, Z., Mou, S., Dong, M., et al. (2013). Activities of principal
1012 photosynthetic enzymes in green macroalga *Ulva linza*: functional implication of C4 pathway in CO_2
1013 assimilation. *Science China Life Sciences*, 56(6), 571–580. https://doi.org/10.1007/s11427-013-
1014 4489-x

1015 Wefer, G., & Berger, W. H. (1981). Stable isotope composition of benthic calcareous algae from
1016 Bermuda. *Journal of Sedimentary Research*, 51(2), 459–465. https://doi.org/10.1306/212F7CAC-
1017 2B24-11D7-8648000102C1865D

1018 Wilkinson T. E., Wiken, J., Bezaury-Creel, T., Hourigan, T., Agardy, H., Herrmann, L., et al. (2009).
1019 Marine Ecoregions of North America. Commission for Environmental Cooperation. Montreal,
1020 Canada. 200 pp.

1021 Zabaleta, E., Martin, M. V., & Braun, H. P. (2012). A basal carbon concentrating mechanism in
1022 plants?. *Plant Science*, 187, 97–104. https://doi.org/10.1016/j.plantsci.2012.02.001

1023 Zeebe, R. E., & Wolf-Gladrow, D. (2001). CO_2 in seawater: equilibrium, kinetics, isotopes (No. 65).
1024 Gulf Professional Publishing.

1025 Zeitzschel, B. (1969). Primary productivity in the Gulf of California. *Marine Biology*, 3(3), 201–
1026 207. https://doi.org/10.1007/BF00360952

1027 Zhou, L., Gao, S., Huan, L., Wu, S., Wang, G., & Gu, W. (2020). Enzyme activities suggest that the
1028 NAD-ME C4 type CCM exist in *Ulva* sp. *Algal Research*, 47, 101809.
1029 https://doi.org/10.1016/j.algal.2020.101809

1030 Zou, D., Xia, J., & Yang, Y. (2004). Photosynthetic use of exogenous inorganic carbon in the

1031 agarophyte *Gracilaria lemaneiformis* (Rhodophyta). *Aquaculture,* 237, 421-31.

1032 https://doi.org/10.1016/j.aquaculture.2004.04.020

1033

1034

1035

1036

1037

1038

Table 1. Carbon isotopic composition (‰) in species of phyla Chlorophyta collected along Gulf of California coastlines.

Species (n composite samples)	$\delta^{13}C\pm SD$ (Min to Max, ‰)
Chaetomorpha sp. (3)	-13.7±0.83 (-14.56 to -12.9)
C. antennina (10)	-14.58±1.10 (-16.29 to -12.79)
C. linum (5)	-16.84±1.65 (-18.45 to -14.6)
Codium sp. (5)	-11.6±3.01 (-14.07 to-6.65)
C. amplivesiculatum (8)	-14.44±2.74 (-20.42 to -11.25)
C. brandegeei (7)	-11.82±1.24 (-13.67 to -10.43)
C. fragile (4)	-13.0±2.66 (-14.78 to -9.04)
C. simulans (9)	-11.4±2.20 (-14.92 to -8.26)
Ulva sp. (12)	-13.98±3.85 (-19.16 to -7.11
U. acanthophora (25)	-15.78±1.72 (-18.27 to -11.44)
U. clathrata (8)	-16.35± 2.01 (-20.54 to -14.52)
U. compressa (4)	-17.84±2.39 (-20.58 to -15.42)
U. flexuosa (13)	-16.03±3.67 (-25.92 to -10.38)
U. intestinalis (16)	-15.29±2.54 (-20.29 to -8.95)
U. lactuca (31)	-14.1±3.14 (-19.56 to -7.67)
U. linza (6)	-15.56±2.44 (-19.43 to -13.21)
U. lobata (5)	-13.18±1.87 (-15.33 to -11.11)
U. prolifera (3)	-14.24±1.76 (-15.49 to -12.22)

1039

Table 2. Carbon isotopic composition (‰) in species of phyla Ochrophyta collected along Gulf of California coastlines.

Species (n composite samples)	$\delta^{13}C \pm SD$ (Min to Max, ‰)
Colpomenia sp. (11)	-10.97±3.65 (-18.98 to -5.42)
C. ramosa (4)	-11.43±2.55 (-13.76 to-7.81)
C. sinuosa (7)	-10.18±2.95 (-16.27 to -7.18)
C. tuberculata (64)	-8.72±3.20 (-19.19 to -2.20)
Padina sp. (15)	-11.1±1.53 (-13.06 to-7.94)
P. crispata (3)	-11.27±1.71 (-12.47 to -10.06)
P. durvillaei (36)	-13.2±2.59 (-19.97 to -9.19)
Sargassum sp. (34)	-14.25±2.36 (-18.71 to -7.95)
S. herporhizum (7)	-13.65±1.63 (-16.59 to -11.51)
S. horridum (12)	-15.52±2.89 (-19.72 to-9.52)
S. johnstonii (10)	-15.41±1.98 (-17.71 to -11.8)
S. lapazeanum (7)	-14.49±1.59 (-17.19 to -12.81)
S. sinicola (31)	-15.11±2.41 (-21.1 to -12.13)

1040

1041   Table 3. Carbon isotopic composition (‰) in species of phyla Rhodophyta collected along Gulf of

1042   California coastlines.

Species (n composite samples)	$\delta^{13}C \pm SD$ (Min to Max, ‰)
Gracilaria sp. (18)	-15.48±2.43 (-21.83 to -12.24)
Gracilaria sp.2 (3)	-14.41±3.71 (-18.7 to -12.26)
G. crispata (7)	-15.07±2.96 (-19.13 to -10.14)
G. pacifica (6)	-16.48±1.64 (-18.57 to -13.61)
G. spinigera (3)	-14.94±3.84 (-17.66 to -12.23)
G. subsecundata (8)	-15.93±2.82 (-20.31 to -12.78)
G. tepocensis (3)	-15.1±1.92 (-17.01 to -13.16)
G. textorii (4)	-16.2±2.62 (-18.05 to -14.35)
G. turgida (5)	-15.34±3.56 (-20.72 to -12.04
G. vermiculophylla (16)	-15.88±3.83 (-23.35 to -8.81)
Hypnea sp. (14)	-14.95±2.56 (-20.85 to -11.41)
H. johnstonii (5)	-11.18±3.52 (-13.76 to -6.54)
H. pannosa (5)	-11.8±3.31 (-14.95 to -6.39)
H. spinella (6)	-16.44±1.75 (-19.23 to -14.87)
H. valentiae (6)	-15.24±2.32 (-19.16 to -12.66)
Laurencia sp. (8)	-12.92±1.22 (-14.65 to -10.95)
L. pacifica (8)	-14.86±2.19 (-18.97 to -12.69)
L. papillosa (3)	-15.75±0.28 (-15.95 to -15.55)
Spyrida sp. (5)	-17.06±1.120 (-19.11 to -16.13)
S. filamentosa (14)	-15.86±3.83 (-26.16 to -11.46)

1043

1044

Table 4. Summary of the estimated regression coefficients for each simple linear regression analyses and on the constant of fitted regression models. Estimated regression coefficients includes degrees of freedom for the error (DFE), root-mean-square error (RMSE), coefficients of determination (R^2) and the adjusted R^2 statistics, Mallow's Cp criterion (Cp), Akaike Information Criterion (AIC), Bayesian Information Criterion (BIC) minimum, F Ratio test, and p-value for the test (Prob > F). Models information includes value of the constant a (δ^{13}C, ‰), standard error (SE), t ratio and Prob > |t| (values * are significant).

Independent variables	DFE	RMSE	R^2	Adjust R^2	Cp	AICc	BIC	F ratio	Prob > F	δ^{13}C (‰)	SE	t ratio	Prob > |t|
									Estimated regression coefficients			**Model constant (a)**	
									Inherent macroalgae properties				
Phyla	806	3.66	0.08	0.07	3	4,401	4,420	33.1	<.0001*	-13.98	0.13	-107.4	<.0001*
Morphofunctional	788	3.10	0.35	0.34	21	4,149	4,251	21.6	<.0001*	-14.21	0.35	-40.80	<.0001*
Genero	746	2.92	0.46	0.41	63	4,104	4,393	10.1	<.0001*	-14.71	0.23	-62.64	<.0001*
Species	641	2.79	0.57	0.46	168	4,195	4,898	5.2	<.0001*	-14.60	0.16	-93.22	<.0001*
									Biogeographical collection zone				
GC coastline	807	3.79	0.01	0.01	2	4,456	4,470	7.4	0.0067*	-13.97	0.13	-104.5	<.0001*
Coastal sector	803	3.73	0.05	0.04	6	4,433	4,465	7.9	<.0001*	-14.12	0.16	-90.85	<.0001*
Latitude	807	3.80	0.00	0.00	2	4,462	4,476	1.5	0.23	-12.25	1.41	-8.71	<.0001*

Longitude	807	3.81	0.00	-0.00	2	4,463	4,477	0.1	0.80	-15.44	5.83	-2.65	0.0082*
Habitat features													
Substrate	807	3.80	0.00	0.00	2	4,460	4,474	3.2	0.08	-13.82	0.15	-92.06	<.0001*
Hydrodynamic	807	3.80	0.00	0.00	2	4,462	4,476	1.3	0.26	-13.88	0.15	-95.00	<.0001*
Emersion level	807	3.69	0.06	0.06	2	4,412	4,427	52.2	<.0001*	-14.05	0.13	-107.6	<.0001*
Environmental conditions													
Temperature	802	3.70	0.01	0.01	2	4,390	4,404	5.4	0.0207*	-16.11	0.96	-16.78	<.0001*
pH	807	3.73	0.04	0.04	2	4,430	4,444	33.4	<.0001*	-32.45	3.21	-10.13	<.0001*
Salinity	806	3.80	0.00	-0.00	2	4,456	4,470	0.9	0.34	-15.77	1.91	-8.27	<.0001*

1050

1051

1052 Table 5. Summary of the estimated regression coefficients for each multivariate linear regression analyses and on their constant of

1053 fitted regression models performed in individuals binned by genus. Estimated regression coefficients include degrees of freedom for

1054 the error (DFE), root-mean-square error (RMSE), coefficients of determination (R^2) and the adjusted R^2 statistics, Mallow's Cp

1055 criterion (Cp), Akaike Information Criterion (AIC), Bayesian Information Criterion (BIC) minimum, F Ratio test, and p-value for the

1056 test (Prob > F). Model information includes value of the constant a ($\delta^{13}C$, ‰), standard error (SE), t ratio and Prob > |t| (values * are

1057 significant).

				Estimated regression coefficients						Model constant (a)			
Independent variables	DFE	RMSE	R^2	Adjust R^2	Cp	AICc	BIC	F ratio	Prob > F	$\delta^{13}C$ (‰)	SE	t ratio	Prob > |t|
Coastal sector	652	2.78	0.57	0.47	157	4,169	4,834	20.0	<.0001*	-17.52	0.64	-27.24	<.0001*
Substrate	711	2.90	0.49	0.42	98	4,140	4,577	0.4	0.52	-16.35	0.62	-26.20	<.0001*
Hydrodynamic	714	2.87	0.50	0.43	95	4,120	4,545	0.1	0.78	-16.53	0.64	-25.95	<.0001*
Emersion level	713	2.77	0.53	0.47	96	4,060	4,489	153.0	<.0001*	-16.65	0.60	-27.85	<.0001*
Temperature	695	2.81	0.50	0.43	109	4,083	4,564	98.4	<.0001*	-14.60	0.92	-15.91	<.0001*
Temperature ranges	686	2.87	0.49	0.40	118	4,128	4,645	97.7	<.0001*	-12.91	0.40	-31.97	<.0001*
pH	701	2.86	0.51	0.43	108	4,134	4,611	156.6	<.0001*	-28.57	2.69	-10.64	<.0001*
pH ranges	697	2.67	0.57	0.51	112	4,028	4,522	152.2	<.0001*	-16.39	0.58	-28.05	<.0001*

Salinity	697	2.89	0.50	0.42	111	4,151	4,640	162.2	<.0001*	-17.75	1.63	-10.88	<.0001*
Salinity ranges	721	2.91	0.47	0.41	86	4,117	4,504	167.8	<.0001*	-17.64	0.74	-23.68	<.0001*

1058

Table 6. Summary of the estimated regression coefficients for each multivariate linear regression analyses and on their constant of fitted regression models performed in individuals binned by coastline sector and genus. Estimated regression coefficients include degrees of freedom for the error (DFE), root-mean-square error (RMSE), coefficients of determination (R^2) and the adjusted R^2 statistics, Mallow's Cp criterion (Cp), Akaike Information Criterion (AIC), Bayesian Information Criterion (BIC) minimum, F Ratio test, and p-value for the test (Prob > F). Model information includes value of the constant a ($\delta^{13}C$, ‰), standard error (SE), t ratio and Prob > |t| (values * are significant).

Independent variables	DFE	RMSE	R^2	Adjust R^2	Cp	AICc	BIC	F ratio	Prob > F	$\delta^{13}C$ (‰)	SE	t ratio	Prob > |t|
Substrate	590	2.76	0.62	0.47	219	4,287	5,155	15.8	<.0001*	-17.08	0.66	-25.72	<.0001*
Hydrodynamic	592	2.73	0.62	0.49	217	4,266	5,128	18.6	<.0001*	-17.18	0.67	-25.70	<.0001*
Protection level	590	2.75	0.62	0.48	219	4,285	5,153	20.0	<.0001*	-17.51	0.64	-27.22	<.0001*
Emersion level	603	2.69	0.63	0.50	206	4,217	5,045	18.6	<.0001*	-17.47	0.64	-27.49	<.0001*
Temperature ranges	569	2.74	0.61	0.46	235	4,293	5,202	28.0	<.0001*	-13.73	0.45	-30.32	<.0001*
pH ranges	580	2.50	0.69	0.57	229	4,155	5,051	9.7	0.0019*	-16.88	0.62	-27.15	<.0001*
Salinity ranges	631	2.76	0.58	0.47	176	4,183	4,913	21.2	<.0001*	-18.30	0.79	-23.05	<.0001*

1066　Table 7. Summary of the estimated regression coefficients for each multivariate linear regression analyses and on their constant of

1067　fitted regression models performed in individuals binned in coastline sector, habitats features, environmental conditions, and

1068　Physiological performed separately by morpho-functional groups and genus. Estimated regression coefficients include degrees of

1069　freedom for the error (DFE), root-mean-square error (RMSE), coefficients of determination (R^2) and the adjusted R^2 statistics,

1070　Mallow's Cp criterion (Cp), Akaike Information Criterion (AIC), Bayesian Information Criterion (BIC) minimum, F Ratio test, and p-

1071　value for the test (Prob > F). Model information includes value of the constant a ($\delta^{13}C$, ‰), standard error (SE), t ratio and Prob > |t|

1072　(values * are significant).

				Estimated regression coefficients							Model constant (a)			
				Adjust					Prob >	$\delta^{13}C$			Prob >
Full model	DFE	RMSE	R^2	R^2	Cp	AICc	BIC	F ratio	F	(‰)	SE	t ratio	|t|
Coastline sector + Habitats features + Morphofunctional group													
I-Morpho-functional	593	2.79	0.60	0.46	216	4,301	5,160	20.8	<.0001*	-13.49	0.57	-23.52	<.0001*
Coastline sector + Environmental conditions + Morphofunctional group													
II-Morpho-functional	680	2.90	0.51	0.42	129	4,189	4,750	25.1	<.0001*	-13.42	0.54	-24.74	<.0001*
Coastline sector + Habitat features+ Genus													
I-Genus	482	2.66	0.71	0.51	327	4,565	5,655	15.8	<.0001*	-16.93	0.73	-23.27	<.0001*
Coastline sector + Environmental conditions + Genus													
II-Genus	494	2.49	0.72	0.55	310	4,374	5,438	14.8	0.0001*	-13.55	0.64	-21.17	<.0001*

1073

1074   Table 8. Constant of fitted regression model explaining the δ^{13}C variability by morpho-functional

1075   groups. Model information includes value of the constant a (δ^{13}C, ‰), standard error (SE), t ratio

1076   and Prob > |t|. Only morpho-functional groups with significant effects are enlisted.

Term	Estimated	SE	Razón t	Prob > |t|
Model constant	-14.21	0.35	-40.80	<.0001*
R-Smaller-sized articulated corallines	4.48	1.74	2.58	0.0100*
O-Compressed with branched or divided thallus	1.24	0.46	2.66	0.0079*
C-Erect thallus	1.76	0.62	2.84	0.0046*
R-Larger-sized articulated corallines	6.32	0.80	7.95	<.0001*
O-Hollow with spherical or subspherical shape	4.96	0.47	10.51	<.0001*
R-Blade-like with one of few layers of cells	-5.89	2.97	-1.98	0.0476*
C-Tubular	-1.62	0.50	-3.26	0.0012*
R-Filamentous uni&pluriseriate with erect thallus	-2.15	0.55	-3.92	<.0001*
R-Flattened macrophytes with cortication	-8.89	1.25	-7.10	<.0001*

1077

1078

1079

1080

1081

1082

1083

1084

1085   Table 9. Constant of fitted regression model explaining the $\delta^{13}C$ variability by genus. Model

1086   information includes value of the constant a ($\delta^{13}C$, ‰), standard error (SE), t ratio and Prob > |t|.

1087   Only genus with significant effects are enlisted.

Term	Estimated	SE	Razón t	Prob > |t|
Model constant	-14.70	0.23	-62.64	<.0001*
Corallina	6.40	2.88	2.22	0.0269*
Tacanoosca	3.54	1.31	2.71	0.0070*
Jania	4.98	1.68	2.97	0.0031*
Struveopsis	4.12	1.31	3.15	0.0017*
Codium	2.26	0.55	4.08	<.0001*
Padina	2.19	0.46	4.8	<.0001*
Hydroclathrus	7.33	1.11	6.59	<.0001*
Amphiroa	6.84	0.76	9.05	<.0001*
Colpomenia	5.45	0.39	14.02	<.0001*
Spyridia	-1.46	0.70	-2.10	0.0361*
Gracilaria	-0.89	0.41	-2.18	0.0294*
Polysiphonia	-3.75	0.78	-4.82	<.0001*
Schizymenia	-19.08	2.05	-9.33	<.0001*

1088
1089

1090 Table 10. Constant of fitted regression model explaining the δ^{13}C variability by species. Model

1091 information includes value of the constant a (δ^{13}C, ‰), standard error (SE), t ratio and Prob > |t|.

1092 Only genus with significant effects are enlisted.

Term	δ^{13}C, ‰ estimated	SE	Razón t	Prob > |t|
Constante del modelo	-14.59	0.16	-93.22	<.0001*
Hypnea pannosa	2.79	1.25	2.24	0.0256*
Colpomenia ramosa	3.16	1.39	2.27	0.0237*
Corallina vancouverensis	6.29	2.78	2.27	0.0238*
Caulerpa peltata	3.86	1.61	2.4	0.0165*
Codium sp.	3.00	1.25	2.4	0.0167*
Amphiroa misakiensis	7.08	2.78	2.55	0.0110*
Jania sp.	5.04	1.97	2.56	0.0106*
Codium brandegeei	2.78	1.06	2.63	0.0088*
Hypnea johnstonii	3.42	1.25	2.74	0.0063*
Tacanoosca uncinata	3.43	1.25	2.74	0.0062*
Struveopsis sp.	3.98	1.39	2.86	0.0044*
Padina durvillaei	1.40	0.49	2.87	0.0043*
Amphiroa sp.*3*	8.20	2.78	2.95	0.0033*
Codium simulans	3.19	0.94	3.41	0.0007*
Amphiroa sp.2	6.59	1.61	4.1	<.0001*
Colpomenia sinuosa	4.42	1.06	4.17	<.0001*

Colpomenia sp.	3.63	0.85	4.27	<.0001*
Padina sp.	3.50	0.73	4.77	<.0001*
Hydroclathrus clathratus	7.22	1.06	6.82	<.0001*
Amphiroa sp.	8.12	0.94	8.67	<.0001*
Colpomenia tuberculata	5.87	0.38	15.45	<.0001*
Spyrida sp.	-2.46	1.25	-1.97	0.0496*
Pyropia thuretii	-5.50	2.78	-1.98	0.0480*
Ulva acanthophora	-1.19	0.58	-2.06	0.0399*
Grateloupia filicina	-2.37	1.14	-2.08	0.0382*
Rhodymenia sp.	-4.08	1.97	-2.08	0.0380*
Ulva compressa	-3.24	1.39	-2.33	0.0203*
Rhizoclonium riparium	-5.06	1.61	-3.15	0.0017*
Polysiphonia sp.	-4.81	1.39	-3.44	0.0006*
Halymenia actinophysa	-9.91	2.78	-3.57	0.0004*
Cladophora microcladioides	-7.16	1.97	-3.64	0.0003*
Polysiphonia mollis	-5.22	1.06	-4.93	<.0001*
Schizymenia pacifica	-19.19	1.97	-9.76	<.0001*

1093
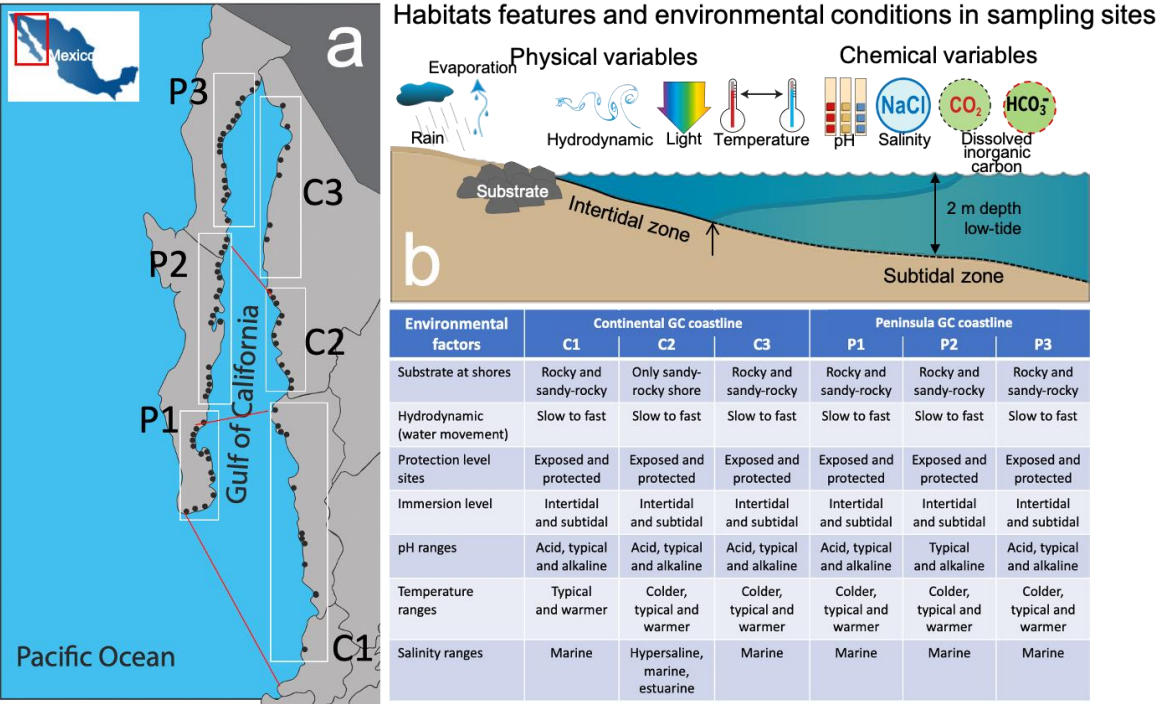1094
1095
1096

1097

1098

1099

Fig. 1. Sites collection along the continental (C1-C3) and peninsula (P1-P3) Gulf of California coastlines (A), range of environmental factors supporting or limiting the life processes for the macroalgal communities within a habitat (B), and inserted Table with the features and environmental conditions in the diverse habitats in the GC ecoregion that delimits the macroalgal community's zonation.
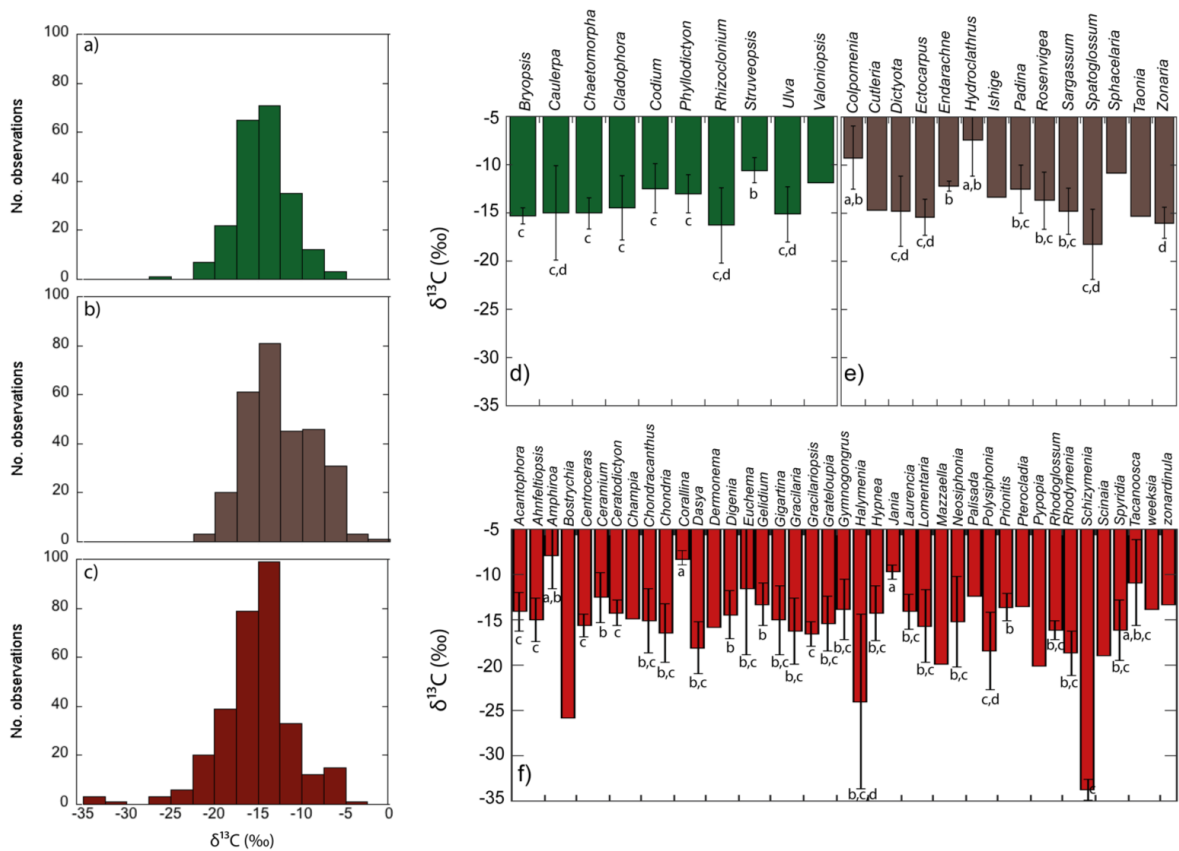
1105

Fig. 2. Variability δ^{13}C values for specimens of different macroalgae genera collected along GC

coastlines classified by taxon, Chlorophyta and Ochrophyta (a) and Rhodophyta (b). Different

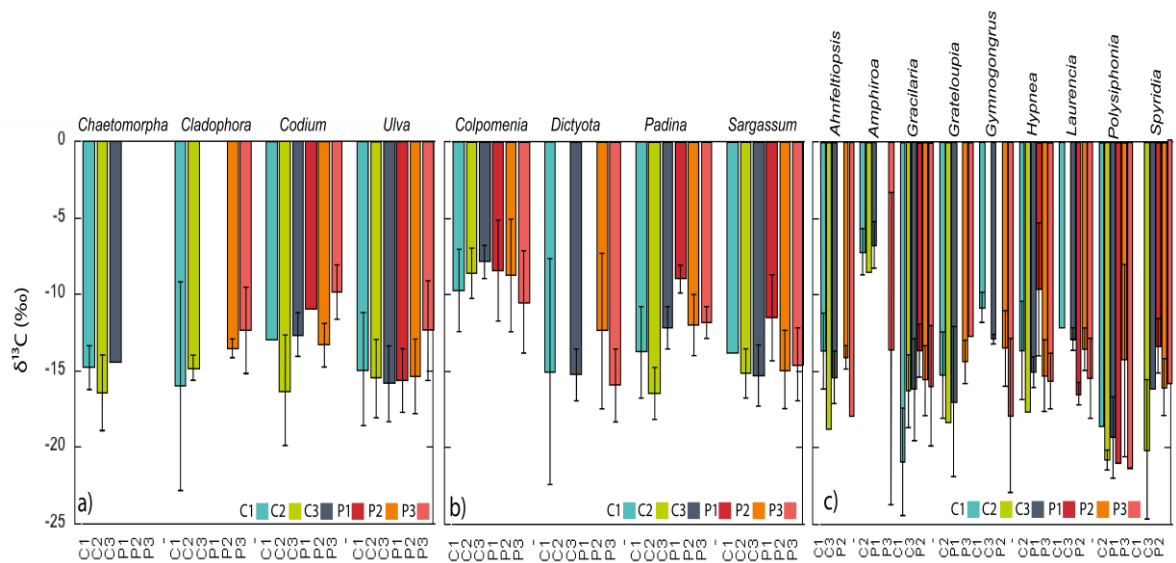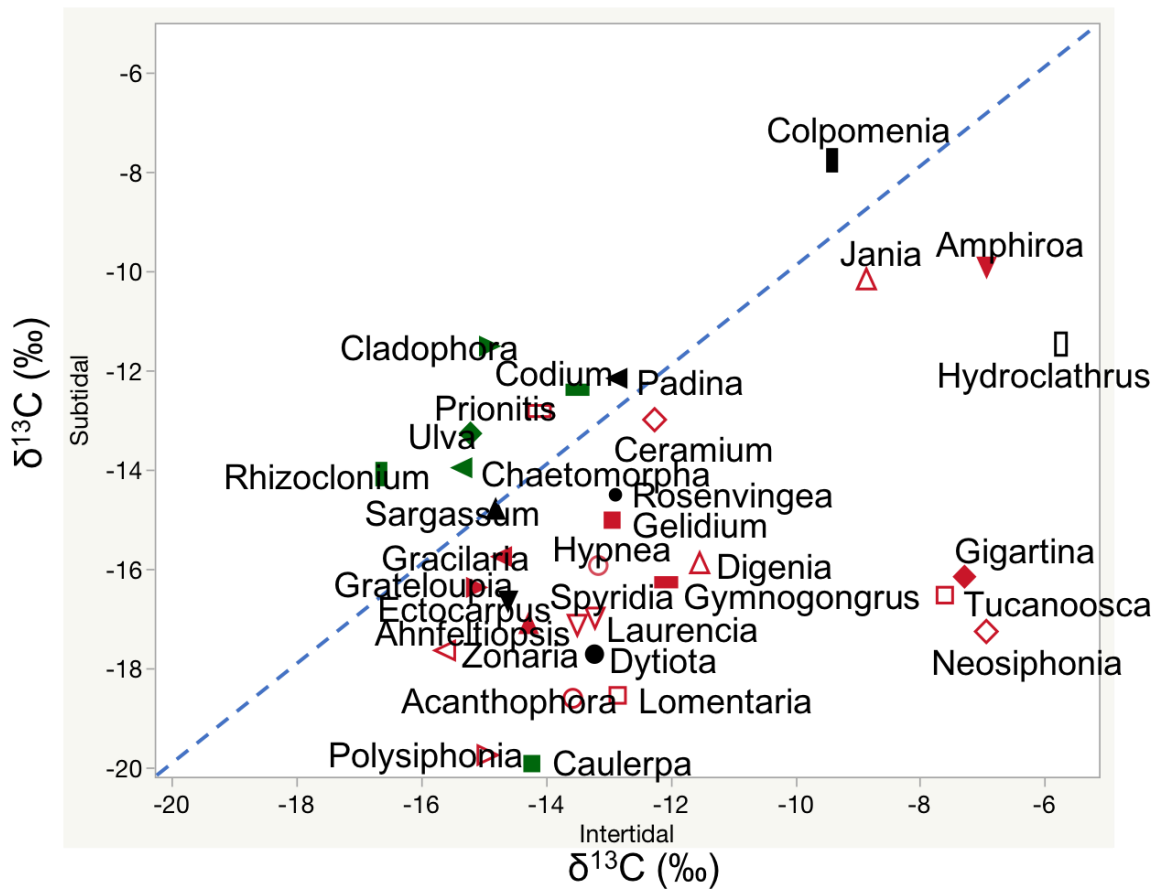letters indicate significant differences (P<0.05): a>b>c>d>e.

1109

59

Fig. 3. Variability δ¹³C values for the most representative genus collected along continental (C1 to C3) and peninsula (P1 to P3) coastline of the Gulf of California.

1114

1115   Fig. 4. Variability of $\delta^{13}C$ values in macroalgae specimens for the most representative genera in

1116   function of habitat features (emersion level).

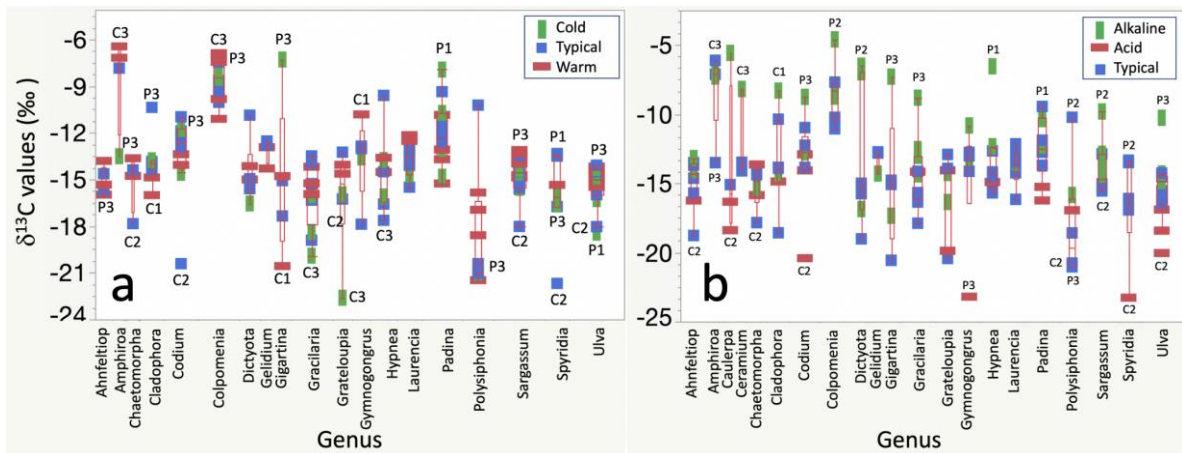1117

Fig. 5. Variability of $\delta^{13}C$ values in macroalgae specimens for the most representative genus in

1118

function of temperature (a) and pH (b) ranges in samples collected along continental (C1-C3) and

1119

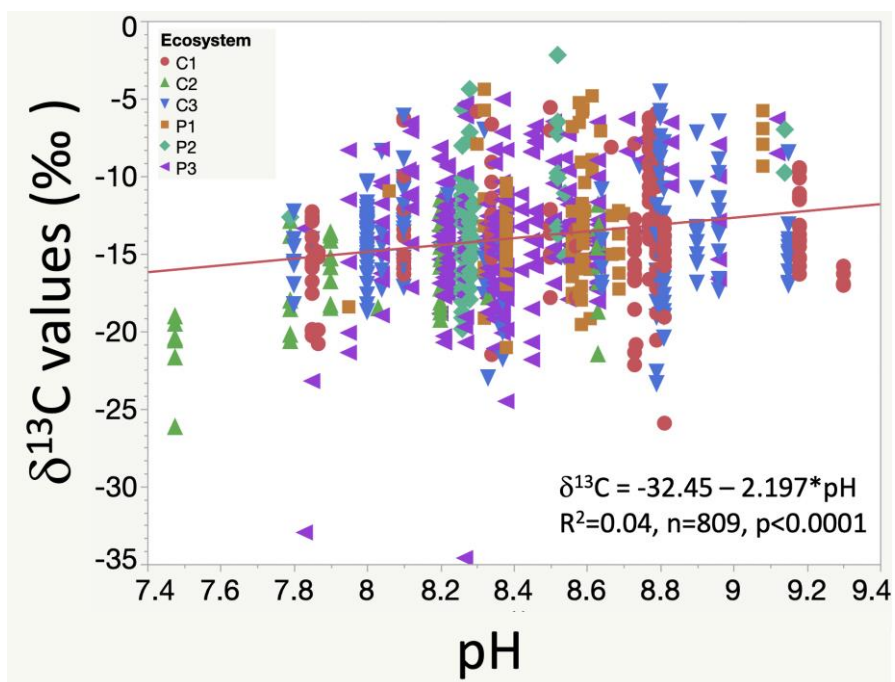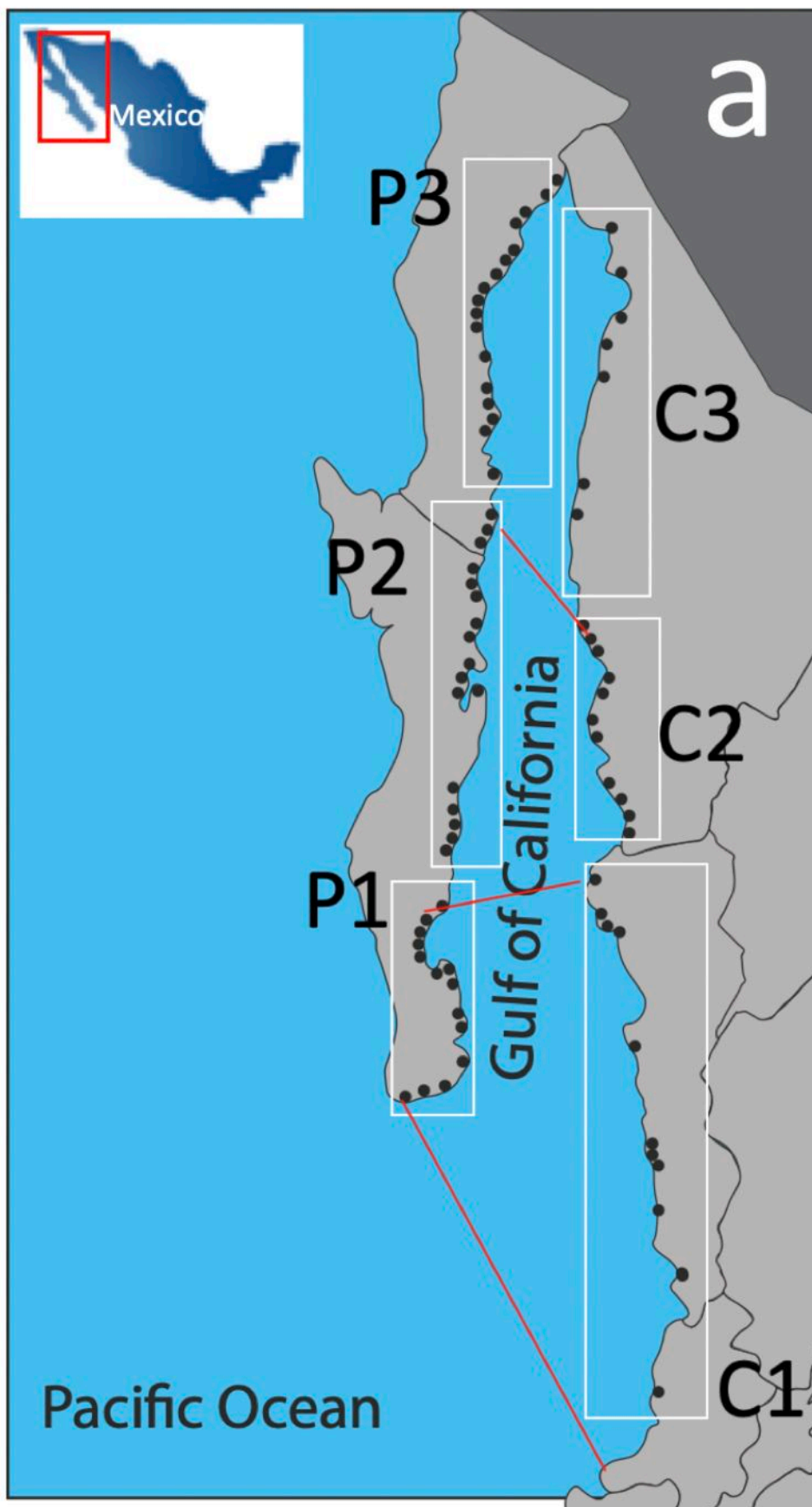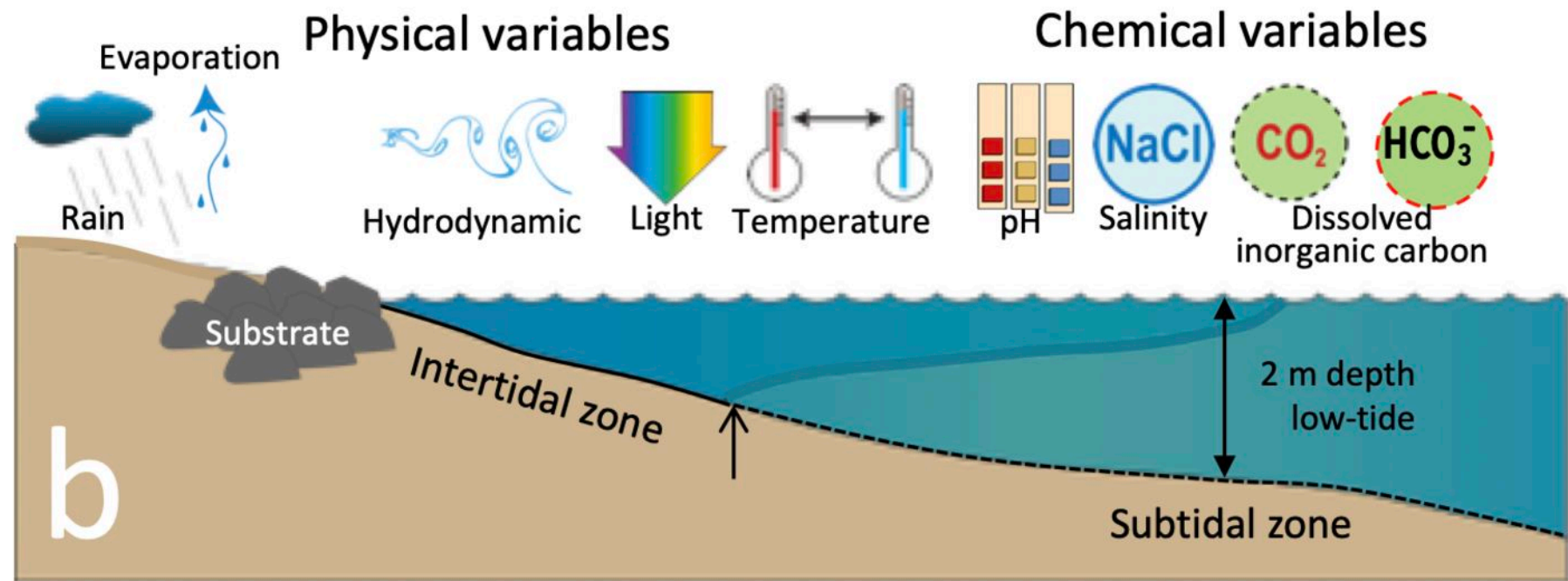peninsula (P1-P3) Gulf of California coastline.

1120

1121

Fig. 6. Trends in the δ^{13}C-macroalgal from GC along latitude gradients for genus classified by phyla Chlorophyta (a), Ochrophyta (b), and Rhodophyta (c). Solid lines indicate the significant relationships with P<0.05.

Fig. 7. Trends in the δ^{13}C-macroalgal in specimens collected along continental (C1-C3) and peninsula (P1-P3) Gulf of California coastline in function of pH in seawater.
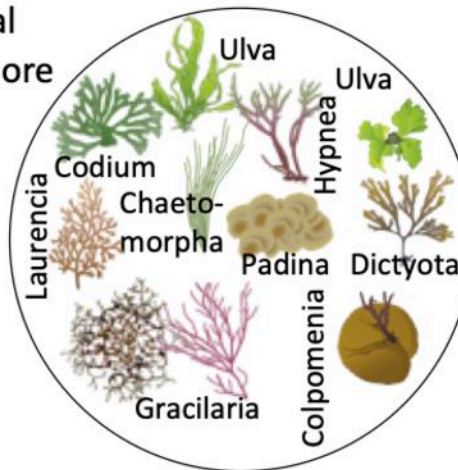
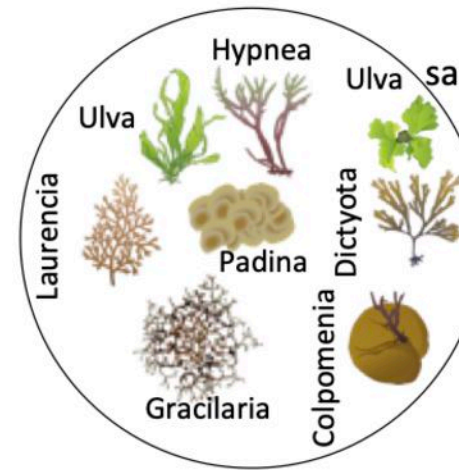**Graphic paper.**

δ^{13}C-macroalgal variability

a Mexico · Pacific Ocean · Gulf of California · P3 · C3 · P2 · C2 · P1 · C1

Habitats features and environmental conditions in sampling sites

Physical variables · Chemical variables

Evaporation · Rain · Hydrodynamic · Light · Temperature · pH · Salinity (NaCl) · Dissolved inorganic carbon (CO_2, HCO_3^-)

b Substrate · Intertidal zone · Subtidal zone · 2 m depth low-tide

Intertidal rocky shore: Ulva, Ulva, Hypnea, Codium, Laurencia, Chaeto-morpha, Padina, Dictyota, Graciliaria, Colpomenia

Intertidal sandy-rocky beach: Hypnea, Ulva, Ulva, Laurencia, Padina, Dictyota, Graciliaria, Colpomenia

Subtidal rocky shore: Acanthophora, Hypnea, Codium, Sargassum, Laurencia, Padina, Dictyota, Graciliaria, Colpomenia

Subtidal sandy-rocky beach: Acanthophora, Hypnea, Laurencia, Sargassum, Padina, Graciliaria, Colpomenia